

# Optimized Tomography of Continuous Variable Systems Using Excitation Counting

Chao Shen,<sup>1</sup> Reinier W. Heeres,<sup>1</sup> Phil Reinhold,<sup>1</sup> Luyao Jiang,<sup>2</sup> Yi-Kai Liu,<sup>3,4</sup> Robert J. Schoelkopf,<sup>1</sup> and Liang Jiang<sup>1</sup>

<sup>1</sup>*Department of Applied Physics, Yale University, New Haven, CT 06511, USA*

<sup>2</sup>*Department of Physics, Yale University, New Haven, CT 06511, USA*

<sup>3</sup>*Joint Center for Quantum Information and Computer Science (QuICS),  
University of Maryland, College Park, MD 20742, USA*

<sup>4</sup>*National Institute of Standards and Technology (NIST), Gaithersburg, MD 20899, USA*

We propose a systematic procedure to optimize quantum state tomography protocols for continuous variable systems based on excitation counting preceded by a displacement operation. Compared with conventional tomography based on Husimi or Wigner function measurement, the excitation counting approach can significantly reduce the number of measurement settings. We investigate both informational completeness and robustness, and provide a bound of reconstruction error involving the condition number of the sensing map. We also identify the measurement settings that optimize this error bound, and demonstrate that the improved reconstruction robustness can lead to an order of magnitude reduction of estimation error with given resources. This optimization procedure is general and can incorporate prior information of the unknown state to further simplify the protocol.

*Introduction.* Quantum state tomography (QST) is a powerful procedure to completely characterize quantum states, which can be extended to quantum process tomography for general quantum operations. However, QST is often resource-consuming, involving preparation of a large number of identical unknown states and measurement of a large set of independent observables. For qubit systems, many techniques have been developed to reduce the cost of full state tomography, such as compressed sensing [1–3], permutationally invariant tomography [4], self-guided/adaptive tomography [5, 6], matrix product states tomography [7]. In contrast, for continuous variable (CV) systems that also play an important role in quantum information, the standard techniques in use today are decades old, namely homodyne measurement [8, 9] for optical photons and direct Wigner function measurement [10–12] for cavity QED. With the rapid development in CV quantum information processing, ranging from arbitrary state preparation [13] to universal quantum control [14, 15] and from engineered dissipation [16, 17] to quantum error correction [18, 19], a large dimension of Hilbert space can be coherently controlled in experiments [12, 20]. However, homodyne measurement might not be immediately applicable due to intrinsic non-linearity preventing applying a very large displacement in cavity QED, and Wigner function measurement requires intensive data collection [20]. Thus there is an urgent need for reliable and efficient tomography for CV systems.

There have been significant advances in excitation counting over various physical platforms, including optical photons [21], microwave photons [22–25], and phonons of trapped ions [26–28]. In particular, the capability of quantum non-demolition measurement of microwave excitation number has been demonstrated with superconducting circuits [29]. Tomography based on ex-

citation counting has also been theoretically proposed [30, 31] and experimentally demonstrated with trapped ions and cavity/circuit QED [25, 26, 32]. However, all these works only considered specific choices of measurement settings (associated with certain displacement patterns), and mostly restricted to the feasibility of tomography, without further investigating the robustness against measurement noise to develop robust QST protocols for CV systems.

Motivated by these recent advances, we develop a theoretical framework to investigate efficient QST protocols for CV systems based on excitation counting. Conventional QST protocols can be regarded as special cases collecting *partial* information of the excitation number distribution. For example, up to a displacement, the Husimi Q function can be regarded as the probability of zero excitation, and the Wigner function can be obtained from the difference between probabilities associated with even and odd number of excitations. We expect more efficient QST by collecting full population distributions upon various displacements using excitation counting, which can be efficiently achieved in various CV systems [21–29].

In this Letter, we first provide a mathematical formulation of QST based on displacements and excitation counting. We then consider QST for a special class of quantum states, illustrating the advantage of excitation counting and introducing the criterion of error robustness in terms of the *condition number* (CN) of the sensing map. Finally, we investigate QST of a general unknown quantum state, and put our optimized scheme to the test using simulated measurement records.

*Informational completeness.* Mathematically, QST solves the inversion problem

$$A \cdot \vec{\rho} = \vec{b},$$

where  $\vec{\rho}$  is the unknown density matrix arranged as a vector,  $\vec{b}$  denotes all the measurement records, and  $A$  is the

sensing matrix determined by the kind of measurements performed. The set of measurements should be *informationally complete* (IC) — that is, the sensing matrix  $A$  should be invertible [33]. For non-square sensing matrix, the unknown state can be reconstructed using least squares fitting,  $\vec{\rho} = \tilde{A}^{-1}\vec{b} = (A^\dagger A)^{-1} A^\dagger \vec{b}$  [34].

For CV systems, each measurement setting is associated with a displacement operation  $D(\beta)$ . We may directly count the excitation number after the displacement operation and obtain the number distribution, which is called the *generalized  $Q$  function* ( $Q_n$  function) [29, 30, 35, 36]

$$Q_n^\beta(\rho) = \text{tr} [|n\rangle \langle n| D(-\beta) \rho D^\dagger(-\beta)]$$

where  $n = 0, 1, 2, \dots, n_c$  with  $n_c$  the maximal resolved excitation number. Reshaping  $\rho$  into a column vector  $\vec{\rho}$  we obtain the linear equation  $\vec{Q}^\beta(\rho) = A^\beta \vec{\rho}$ , where  $\vec{Q}^\beta(\rho)$  is a column vector with  $(n_c + 1)$  entries  $Q_n^\beta(\rho)$  and the matrix  $A^\beta$  has  $(n_c + 1)$  rows. Multiple measurement settings associated with a set of displacements  $\{\beta_1, \beta_2, \dots, \beta_{N_\beta}\}$  are used to constrain the inversion problem. The measurement record  $\vec{b}$  is then a column vector with  $N_\beta \cdot (n_c + 1)$  entries of  $Q_n^{\beta_j}(\rho)$ ; the sensing matrix  $A$  can be obtained by stacking  $A^{\beta_i}$ , with a total of  $N_\beta \cdot (n_c + 1)$  rows. The basis under which  $\rho$  is written can be arbitrary, e.g. Fock basis  $|m_1\rangle \langle m_2|$  or coherent state basis  $|\alpha_i\rangle \langle \alpha_j|$ .

In comparison, the sensing matrix for standard QST with the Husimi  $Q$  function  $Q_{n=0}^\beta(\rho) = \langle \beta | \rho | \beta \rangle$  or Wigner function  $W^\beta(\rho) = \sum_n (-1)^n Q_n^\beta(\rho)$  consists of only  $N_\beta$  rows (which are linear combinations of  $N_\beta \cdot (n_c + 1)$  rows of the sensing matrix associated with  $Q_n$  function [37]), which neglect a large portion of potentially useful information. In the following, we consider QST for a class of quantum states and show that the neglected information can be crucial.

**QST for cat states.** Cat states are quantum states characterized by density matrix  $\rho = \sum_{i,j=1}^p \rho_{ij} |\alpha_i\rangle \langle \alpha_j|$ , where  $|\alpha_i\rangle$  are well separated coherent states [38]. The Schrödinger cat state  $|\alpha\rangle + |-\alpha\rangle$  is a well-known example. Standard QST of cat states with large unknown  $\alpha$ 's is resource consuming and requires many measurement settings. In particular, both the Husimi and Wigner function measurement schemes encounter the challenge of unknown  $\alpha$ 's, and have to deploy many measurement settings to scan various displacements, the majority of which is unfortunately wasted because  $Q^\beta(\rho) \approx W^\beta(\rho) \approx 0$  for most choices of  $\beta$ . In contrast, the  $Q_n$  function measurement always generates an excitation distribution, from which we can estimate the distances  $|\alpha_i - \beta|$  for different  $\beta$ . Using trilateration, we can estimate all  $\alpha$ 's using about *three* measurement settings (Sec. E of [39]).

Moreover, once the  $\alpha$ 's are known, the generalized  $Q$  function measurement only requires *one additional* measurement setting to fulfill the IC requirement, indepen-

dent of the number of coherent components [40], which can be justified by the relation

$$Q_n^\beta(\rho) = \sum_{i,j=0}^p \rho_{ij} Q_n^\beta(|\alpha_i\rangle \langle \alpha_j|) = \sum_{i,j=0}^p \tilde{\rho}_{ij} \frac{1}{n!} [d_i d_j e^{i\phi_{ij}}]^n,$$

where  $d_i \equiv |\alpha_i - \beta|$ ,  $\phi_{ij} \equiv \arg(\alpha_i - \beta) - \arg(\alpha_j - \beta)$ ,  $\tilde{\rho}_{ij} \equiv e^{i\theta(\beta, \alpha_i, \alpha_j)} e^{-\frac{1}{2}(d_i - d_j)^2} e^{-d_i d_j} \rho_{ij}$  and  $\theta(\beta, \alpha_i, \alpha_j) \equiv -i(-\beta \alpha_i^* + \beta^* \alpha_i - \alpha_j \beta^* + \alpha_j^* \beta)/2$  (as derived in Sec. C of [39]). Reshaping  $\tilde{\rho}_{ij}$  as a column vector, we have

$$\begin{pmatrix} 1 & \cdots & 1 & \cdots \\ \vdots & \ddots & \vdots & \\ d_1^{2n} & \cdots & (d_i d_j e^{i\phi_{ij}})^n & \\ \vdots & & \vdots & \ddots \end{pmatrix} \begin{pmatrix} \tilde{\rho}_{11} \\ \vdots \\ \tilde{\rho}_{ij} \\ \vdots \end{pmatrix} = \begin{pmatrix} 0! Q_0^\beta \\ \vdots \\ n! Q_n^\beta \\ \vdots \end{pmatrix}.$$

The matrix on the left hand side is a Vandermonde matrix, having full column rank (all column vectors are independent and  $A^\dagger A$  is invertible) if and only if all  $d_i d_j e^{i\phi_{ij}}$  are distinct [41]. The  $Q_n$  function at one suitable  $\beta$  contain sufficient information. More specifically, the diagonal terms in the density matrix  $\rho_{ii}$  (the population of  $|\alpha_i\rangle$ ) can be extracted from the envelope of the distribution, while the off-diagonal terms  $\rho_{i,j}$  can be obtained from the interference signals peaked at  $\tilde{n} = d_i d_j$  in the distribution. Therefore, sampling the excitation number distribution can boost the information gain and thus reduce the measurement settings significantly.

So far, we have only considered the requirement for IC, possibility of reconstruction. We do not yet know the accuracy of the reconstruction when measurements are noisy. Next, we investigate robustness and estimate the reconstruction error.

**Error robustness of reconstruction.** In practice, the measurements  $\vec{b}$  have noise  $\delta \vec{b}$ , leading to noise in the solution  $\tilde{A}^{-1} \delta \vec{b}$ . To bound the noise in the solution, we consider the worst-case noise magnification ratio

$$\kappa(A) \equiv \frac{\|\tilde{A}^{-1} \delta \vec{b}\| / \|\tilde{A}^{-1} \vec{b}\|}{\|\delta \vec{b}\| / \|\vec{b}\|},$$

which is called the *condition number* (CN) of  $A$  [42]. The CN is a property of the sensing map and does not depend on the specific procedure that solves the linear equations. For the 2-norm  $\|\bullet\|_2$  of vectors, the CN is simply the ratio of the largest and smallest singular values of  $A$  [42]. Clearly  $\kappa(A) \geq 1$  and when  $\kappa(A) = 1$  the sensing map is isometric (distance preserving). The CN has been introduced as a measure of robustness of reconstruction schemes for qubit systems [43–45]. Using Uhlmann's definition  $F(\rho, \sigma) = \text{Tr} [\sqrt{\sqrt{\rho} \sigma \sqrt{\rho}}]$ , the reconstruction fidelity can be bounded as (Sec. B of [39])

$$F(\rho, \rho + \delta \rho) \geq 1 - \frac{1}{2} \kappa(A) \sqrt{r} \|\rho\|_F \|\delta \vec{b}\| / \|\vec{b}\|, \quad (1)$$

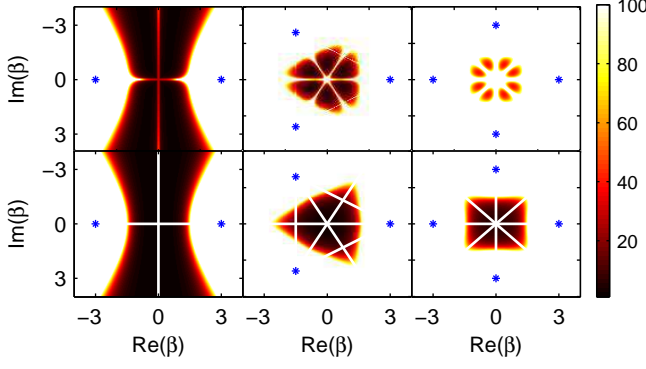


Figure 1. (Color online) Condition number of the sensing map as a function of  $\beta$  for cat states with number of components  $p = 2, 3, 4$ . **Upper panels:** numerical results for CN; **Lower panels:** a simple estimate of the CN using the expression  $\kappa(\beta) \sim \sum_{i,j} \exp[(d_i - d_j)^2 / 2]$  where  $d_i \equiv |\alpha_i|$ . We also included the white lines on which the sensing map is strictly informationally incomplete, see main text. Blue stars indicate the positions of the coherent components  $|\alpha_i\rangle$ . For visual clarity, values beyond 100 are all mapped to white. The minimum CN achievable for the three cases are 1.74, 6.81 and 38.64 (numerical results), respectively. Here the maximal resolved excitation number  $n_c$  is taken sufficiently large. If  $n_c$  is decreased, CN for large  $|\beta|$  gets worse.

where  $r$  is the rank of  $\delta\rho$  and  $\|\rho\|_F$  is the Frobenius norm of the density matrix, which are fixed parameters. Assuming for now that  $\|\delta\vec{b}\| / \|\vec{b}\|$  is fixed (e.g., due to systematic bias), a robust QST should minimize CN to have an optimal guarantee of the reconstruction fidelity.

We now use the CN to examine the robustness of QST for cat-states, for which CN is a function of one complex variable  $\kappa(\beta)$ . Due to the factor  $e^{-\frac{1}{2}(d_i - d_j)^2}$  in  $Q_n^\beta(|\alpha_i\rangle\langle\alpha_j|)$ , we expect that when  $d_i \ll d_j$  or  $d_i \gg d_j$ ,  $\rho_{ij}$  gets exponentially suppressed, just like the case with the Husimi Q function. In those regions, the factor  $\exp[(d_i - d_j)^2 / 2]$  would magnify the noise during the reconstruction. Thus we estimate  $\kappa(\beta) \sim \sum_{i,j} \exp[(d_i - d_j)^2 / 2]$ , which agrees well with the numerical calculation of CN, as illustrated in Fig. 1. Different from the requirement for IC, CN depends on the number of coherent components  $p$ , the values of  $\alpha_i$ , and the choice of  $\beta$ . For small  $p$ , there exists low-CN regions of  $\beta$  (dark regions in Fig. 1), which implies that the protocol with only about four measurement settings (about three for trilateration and one for coherences) can be robust. These low-CN regions are very similar to the regions with high Fisher information in the worst case (Sec. G of [39]). This justifies the use of CN as a guide for optimizing measurement schemes, which is much easier to calculate than the worst-case Fisher information. For larger  $p$  or general states, we need to consider multiple measurement settings and optimized choices of  $\beta$ 's

as discussed below.

*IC for general states.* We now consider general states with no structure other than an excitation number cutoff  $m_c$ . To achieve IC, we need  $N_\beta = (m_c + 1)$  different  $\beta$ 's. In Fock basis,  $\rho = \sum_{m_1, m_2=0}^{m_c} \rho_{m_1, m_2} |m_1\rangle\langle m_2|$ , and for each term  $|m_1\rangle\langle m_2|$

$$Q_n^\beta(|m_1\rangle\langle m_2|) = \frac{|\beta|^{2n} e^{-|\beta|^2}}{n!} \frac{\sqrt{m_1! m_2!}}{(-\beta)^{m_1} (-\beta^*)^{m_2}} \mathcal{L}_{m_1}^{n-m_1}(|\beta|^2) \mathcal{L}_{m_2}^{n-m_2}(|\beta|^2),$$

where  $\mathcal{L}_m^n(x)$  is the associated Laguerre polynomial. Note that  $\mathcal{L}_m^n(x)$  is not only a polynomial of degree  $m$  in  $x$  but also a polynomial of degree  $m$  in  $n$ . Apart from the factor  $\frac{|\beta|^{2n} e^{-|\beta|^2}}{n!}$ ,  $Q_n^\beta(|m_1\rangle\langle m_2|)$  is a polynomial of degree  $(m_1 + m_2)$  in  $n$ . Since  $Q_n^\beta(\rho)$  has a degree of  $2m_c$  in  $n$ , measurement of  $Q_n^{\beta_1}(\rho)$  provides  $(2m_c + 1)$  real coefficients, among which the coefficient of  $n^{2m_c}$  reveals  $\rho_{m_c, m_c}$  and the coefficient of  $n^{2m_c-1}$  gives a linear equation involving  $\rho_{m_c, m_c-1}$  and  $\rho_{m_c-1, m_c}$ . After measuring  $Q_n^{\beta_2}(\rho)$  the values of  $\rho_{m_c, m_c-1}$  and  $\rho_{m_c-1, m_c}$  can be determined. Continuing this way we can determine all of  $\rho_{m_1, m_2}$  after measuring  $Q_n^\beta(\rho)$  for  $(m_c + 1)$   $\beta$ 's (Sec. H of [39]).

*Error robustness for general states.* To analyze CN, it is convenient to consider the covariance matrix,  $C \equiv A^\dagger A = \sum_j A_{\beta_j}^\dagger A_{\beta_j}$ , and  $\kappa(C) = \kappa(A)^2$ . The element  $C_{(m_1 m_2), (n_1 n_2)}$  is the overlap of the columns of  $A$  corresponding to  $|m_1\rangle\langle m_2|$  and  $|n_1\rangle\langle n_2|$ . We find that  $C_{(m_1 m_2), (n_1 n_2)} = \sum_j \beta_j^{m_1 - m_2 - n_1 + n_2} f_{m_1, m_2, n_1, n_2}(|\beta_j|)$  where  $f_{m_1, m_2, n_1, n_2}(|\beta_j|)$  depends only on the magnitudes  $|\beta_j|$  (Sec. D of [39]). Consider a set of  $\beta$ 's with the same magnitude,  $\beta_j = |\beta| e^{i\phi_j}$ . Partitioning the indices  $(m_1 m_2)$  and  $(n_1 n_2)$  into groups according to  $k_1 \equiv m_1 - m_2$  and  $k_2 \equiv n_1 - n_2$ ,  $C$  has a block structure  $C = [C_{k_1 k_2}]$ , where elements of the block  $C_{k_1 k_2}$  are proportional to  $\sum_j e^{-i(k_1 - k_2)\phi_j}$ .

To eliminate all the off-diagonal blocks with  $k_1 \neq k_2$  (known as “pinching” in matrix analysis), we may use  $N_\beta = (2m_c + 1)$  measurement settings with  $\beta$ 's evenly distributed over a circle with  $\phi_j = \frac{2\pi}{2m_c + 1} j$  for  $j = 0, 1, \dots, 2m_c$  (called “full-ring configuration” or FRC, shown in inset of Fig. 2). Due to the pinching-majorization relation, FRC generally improves the CN and in fact we can prove that multiple-FRC scheme can give the optimal CN. Numerically we find that usually a single-FRC with large enough radius is already optimal (Sec. K of [39]). With a smaller  $N_\beta$  it is not possible to satisfy  $\sum_j e^{-i(k_1 - k_2)\phi_j} \propto \delta_{k_1 k_2}$  for all  $k_1, k_2$ . This justifies the ring based configurations used in [25, 26, 30].

Numerically, however, we find that for large  $|\beta|$ , the number of measurement settings can be further reduced from  $2m_c + 1$  to  $m_c + 1$  without compromising CN, as illustrated in Fig. 2. The optimized  $\beta$ 's are evenly distributed over half a circle, with  $\phi_j = \frac{\pi}{m_c + 1} j$  for  $j = 0, 1, \dots, m_c$

(denoted “half-ring configuration” or HRC, as shown in inset of Fig. 2). [46] The justification of HRC lies in the special asymptotic behavior of matrix  $C$ . For  $|\beta|^2 \gtrsim m_c$  the off-diagonal blocks of  $C_{k_1, k_2}$  with odd  $k_1 - k_2$  is negligible to the leading order of  $1/|\beta|$  (Sec. K of [39]), and consequently the pinching condition only requires  $\sum_j e^{-i(k_1 - k_2)\phi_j} \propto \delta_{k_1 k_2}$  for even  $k_1 - k_2$ , which can be achieved using  $m_c + 1$  settings. Interestingly, we found that the matrix  $C$  for  $Q_n$  asymptotes to that of Homodyne detection and hence the optimal angles for Homodyne tomography are also  $\phi_j = \frac{\pi}{m_c + 1}j$  (Sec. L of [39]).

We also performed numerical gradient-based optimization of  $\kappa(A)$  over  $\beta$ 's with different  $N_\beta$ . The gradient of CN with respect to  $\beta$ 's can be calculated using perturbation theory (detailed in Sec. I of [39]). CN drops significantly as  $N_\beta$  increases to  $m_c + 1$  and does not improve further when  $N_\beta > m_c + 1$ . For each  $N_\beta$  we initialize the optimization with a large number of different configurations of  $\beta$ 's and HRC turns out the best (with the exception of the case  $m_c = 1$ ). As a function of  $m_c$ , the asymptotic CN grows slowly,  $\kappa(A) \sim m_c^{1/2}$  (Sec K of [39]).

*Discussion of noise models.* So far, we have assumed that  $\|\delta\vec{b}\| / \|\vec{b}\|$  be fixed, and minimize  $\kappa(A)$  to optimize the bound in Eq. (1). On the other hand,  $\|\delta\vec{b}\| / \|\vec{b}\|$  might be tunable. A practically relevant situation is shot-noise, with  $\|\delta\vec{b}\| / \|\vec{b}\| \propto 1/\sqrt{N_{rep}}$  depending on the number of repetitions  $N_{rep}$ . Meanwhile,  $\kappa(A)$  depends on the number of measurement settings  $N_\beta$ . Given total number of measurements (or copies of unknown states)  $N_{tot} = N_\beta \cdot N_{rep}$ , we need to minimize  $\tilde{\epsilon} \equiv \kappa(A) \|\delta\vec{b}\| / \|\vec{b}\|$  to have a better bound. Hence,

$$\tilde{\epsilon} \propto \kappa(A) / \sqrt{N_{rep}} = \kappa(A) \sqrt{N_\beta / N_{tot}}$$

implies that we should minimize  $\kappa(A) \sqrt{N_\beta}$ . As illustrated in the bottom inset of Fig. 2, having lower  $\kappa(A) \sqrt{N_\beta}$  for large  $|\beta|$ , HRC is more robust than FRC. In terms of scaling with  $m_c$ ,  $\kappa(A) \sqrt{N_\beta} \sim m_c^{1/2} \sqrt{m_c + 1} \sim m_c$  for HRC and FRC while  $\kappa(A) \sqrt{N_\beta}$  appears super-linear in  $m_c$  for Wigner tomography (Sec. L of [39]). The relative advantage of  $Q_n$  tomography grows as  $m_c$  increases.

*Benchmarking with Simulated Data.* Using simulated data (shot-noise only), we test and compare several reconstruction schemes, including Wigner measurements where  $\beta$ 's form a square lattice (yellow triangles), Wigner measurements with optimized  $\beta$ 's (red squares), and  $Q_n$  measurements with optimized  $\beta$ 's (blue circles). For each case the reconstruction can be obtained by fitting a physical density matrix to the data, a semidefinite program that can be solved efficiently with the Matlab package

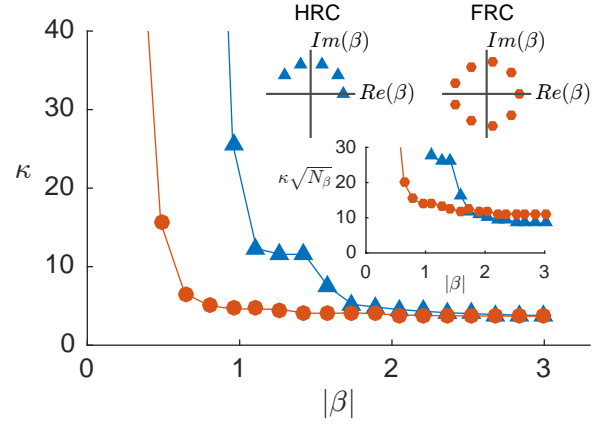


Figure 2. (Color online) **Main panel** shows condition numbers of full-ring configuration (FRC) and half-ring configuration (HRC) as a function of the ring radius ( $m_c = 4$  case). **Top two insets** show FRC and HRC in phase space. For both schemes,  $\beta_j = |\beta| e^{i\phi_j}$ . FRC:  $\phi_j = \frac{2\pi}{2m_c+1}j$ ,  $j = 0, 1, 2, \dots, 2m_c$ ; HRC:  $\phi_j = \frac{\pi}{2m_c+1}j$ ,  $j = 0, 1, 2, \dots, m_c$ . The condition number of HRC approaches that of FRC as  $|\beta|$  gets large, as predicted by theory. **Bottom inset** shows the figure of merit  $\kappa\sqrt{N_\beta}$  for HRC and FRC.

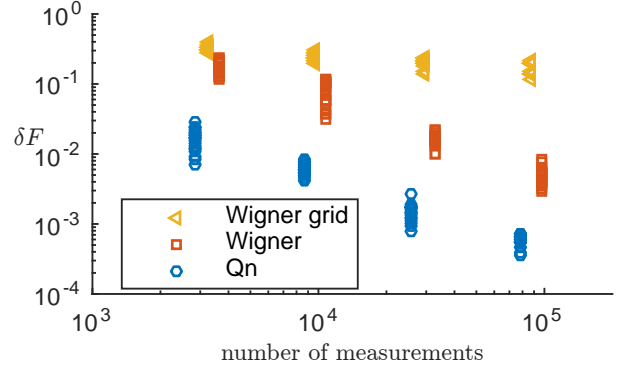


Figure 3. (Color online) Comparison of performances of Wigner measurements where  $\beta$ 's form a square lattice (yellow triangles), Wigner measurements with optimized measurement settings obtained from gradient search (red squares), and  $Q_n$  measurements with optimized measurement settings (blue circles). The true state  $\rho$  is a randomly generated density matrix with excitation number cutoff  $m_c = 5$ . Each scatter point corresponds to one reconstruction based on a set of simulated measurement records containing only shot-noise. The y-axis shows the reconstruction infidelity  $\delta F = 1 - F(\rho, \rho')$  and the x-axis shows the total number of measurements performed, i.e. total number of copies of unknown states consumed.

CVX [47, 48]. A typical case with  $m_c = 5$  is shown in Fig. 3. Both optimized schemes have better error scaling than the unoptimized one, because the bound for the unoptimized case is too forgiving to suppress reconstruction error. Between the two optimized schemes, the reconstruction infidelity for the  $Q_n$ -based scheme is at least



an order of magnitude smaller than that of the Wigner-based scheme. Moreover, the advantage of using  $Q_n$  measurement indeed becomes more significant for larger  $m_c$ , as predicted by the figure of merit (Sec. L of [39]).

*Conclusion and Outlook.* We proposed a procedure to construct an economic set of measurements and identified such a set for  $Q_n$  measurements. Our scheme can be extended to QST scenario where measurements are parameterized by a few CVs. For example, “generalized cat states” reconstruction, where the coherent components are distorted by noise (Sec. M of [39]). Generalizations to multi-oscillator QST, spin ensembles [49] and CV process tomography may greatly reduce resource costs.

We acknowledge support from the AFOSR MURI, ARO, ARL CDQI, the Packard Foundation and the Alfred P. Sloan Foundation. We thank Siddharth Prabhu, Jianming Wen for fruitful discussions.

- 
- [1] D. Gross, Y.-K. Liu, S. T. Flammia, S. Becker, and J. Eisert, *Phys. Rev. Lett.* **105**, 150401 (2010).
  - [2] S. T. Flammia, D. Gross, Y.-K. Liu, and J. Eisert, *New Journal of Physics* **14**, 095022 (2012).
  - [3] A. Kalev, R. L. Kosut, and I. H. Deutsch, *Npj Quantum Information* **1**, 15018 EP (2015), article.
  - [4] G. Tóth, W. Wieczorek, D. Gross, R. Krischek, C. Schwemmer, and H. Weinfurter, *Phys. Rev. Lett.* **105**, 250403 (2010).
  - [5] C. Ferrie, *Phys. Rev. Lett.* **113**, 190404 (2014).
  - [6] D. H. Mahler, L. A. Rozema, A. Darabi, C. Ferrie, R. Blume-Kohout, and A. M. Steinberg, *Phys. Rev. Lett.* **111**, 183601 (2013).
  - [7] M. Cramer, M. B. Plenio, S. T. Flammia, R. Somma, D. Gross, S. D. Bartlett, O. Landon-Cardinal, D. Poulin, and Y.-K. Liu, *Nat Commun* **1**, 149 (2010).
  - [8] K. Vogel and H. Risken, *Phys. Rev. A* **40**, 2847 (1989).
  - [9] D. Sych, J. Řeháček, Z. Hradil, G. Leuchs, and L. L. Sánchez-Soto, *Phys. Rev. A* **86**, 052123 (2012).
  - [10] L. G. Lutterbach and L. Davidovich, *Phys. Rev. Lett.* **78**, 2547 (1997).
  - [11] P. Bertet, A. Auffeves, P. Maioli, S. Osnaghi, T. Meunier, M. Brune, J. M. Raimond, and S. Haroche, *Phys. Rev. Lett.* **89**, 200402 (2002).
  - [12] B. Vlastakis, G. Kirchmair, Z. Leghtas, S. E. Nigg, L. Frunzio, S. M. Girvin, M. Mirrahimi, M. H. Devoret, and R. J. Schoelkopf, *Science* **342**, 607 (2013).
  - [13] M. Hofheinz, H. Wang, M. Ansmann, R. C. Bialczak, E. Lucero, M. Neeley, A. D. O’Connell, D. Sank, J. Wenner, J. M. Martinis, and A. N. Cleland, *Nature* **459**, 546 (2009).
  - [14] S. Krastanov, V. V. Albert, C. Shen, C.-L. Zou, R. W. Heeres, B. Vlastakis, R. J. Schoelkopf, and L. Jiang, *Phys. Rev. A* **92**, 040303 (2015).
  - [15] R. W. Heeres, B. Vlastakis, E. Holland, S. Krastanov, V. V. Albert, L. Frunzio, L. Jiang, and R. J. Schoelkopf, *Phys. Rev. Lett.* **115**, 137002 (2015).
  - [16] M. Mirrahimi, Z. Leghtas, V. V. Albert, S. Touzard, R. J. Schoelkopf, L. Jiang, and M. H. Devoret, *New Journal of Physics* **16**, 045014 (2014).
  - [17] Z. Leghtas, S. Touzard, I. M. Pop, A. Kou, B. Vlastakis, A. Petrenko, K. M. Sliwa, A. Narla, S. Shankar, M. J. Hatridge, M. Reagor, L. Frunzio, R. J. Schoelkopf, M. Mirrahimi, and M. H. Devoret, *Science* **347**, 853 (2015).
  - [18] Z. Leghtas, G. Kirchmair, B. Vlastakis, R. J. Schoelkopf, M. H. Devoret, and M. Mirrahimi, *Phys. Rev. Lett.* **111**, 120501 (2013).
  - [19] N. Ofek, A. Petrenko, R. Heeres, P. Reinhold, Z. Leghtas, B. Vlastakis, Y. Liu, L. Frunzio, S. M. Girvin, L. Jiang, M. Mirrahimi, M. H. Devoret, and R. J. Schoelkopf, nature, accepted (2016).
  - [20] C. Wang, Y. Y. Gao, P. Reinhold, R. W. Heeres, N. Ofek, K. Chou, C. Axline, M. Reagor, J. Blumoff, K. M. Sliwa, L. Frunzio, S. M. Girvin, L. Jiang, M. Mirrahimi, M. H. Devoret, and R. J. Schoelkopf, *Science* **352**, 1087 (2016).
  - [21] B. Calkins, P. L. Mennea, A. E. Lita, B. J. Metcalf, W. S. Kolthammer, A. Lamas-Linares, J. B. Spring, P. C. Humphreys, R. P. Mirin, J. C. Gates, P. G. R. Smith, I. A. Walmsley, T. Gerrits, and S. W. Nam, *Opt. Express* **21**, 22657 (2013).
  - [22] S. Haroche and J.-M. Raimond, *Exploring the Quantum: Atoms, Cavities, and Photons* (Oxford University Press, New York, 2006).
  - [23] M. Brune, F. Schmidt-Kaler, A. Maali, J. Dreyer, E. Hagley, J. M. Raimond, and S. Haroche, *Phys. Rev. Lett.* **76**, 1800 (1996).
  - [24] C. Guerlin, J. Bernu, S. Deleglise, C. Sayrin, S. Gleyzes, S. Kuhr, M. Brune, J.-M. Raimond, and S. Haroche, *Nature* **448**, 889 (2007).
  - [25] H. Wang, M. Hofheinz, M. Ansmann, R. C. Bialczak, E. Lucero, M. Neeley, A. D. O’Connell, D. Sank, M. Weides, J. Wenner, A. N. Cleland, and J. M. Martinis, *Phys. Rev. Lett.* **103**, 200404 (2009).
  - [26] D. Leibfried, D. M. Meekhof, B. E. King, C. Monroe, W. M. Itano, and D. J. Wineland, *Phys. Rev. Lett.* **77**, 4281 (1996).
  - [27] S. An, J.-N. Zhang, M. Um, D. Lv, Y. Lu, J. Zhang, Z.-Q. Yin, H. T. Quan, and K. Kim, *Nat Phys* **11**, 193 (2015), article.
  - [28] H.-Y. Lo, D. Kienzler, L. de Clercq, M. Marinelli, V. Negnevitsky, B. C. Keitch, and J. P. Home, *Nature* **521**, 336 (2015), letter.
  - [29] G. Kirchmair, B. Vlastakis, Z. Leghtas, S. E. Nigg, H. Paik, E. Ginossar, M. Mirrahimi, L. Frunzio, S. M. Girvin, and R. J. Schoelkopf, *Nature* **495**, 205 (2013).
  - [30] T. Opatrny and D.-G. Welsch, *Phys. Rev. A* **55**, 1462 (1997).
  - [31] S. Mancini, P. Tombesi, and V. I. Man’ko, *EPL (Europhysics Letters)* **37**, 79 (1997).
  - [32] S. Deleglise, I. Dotsenko, C. Sayrin, J. Bernu, M. Brune, J.-M. Raimond, and S. Haroche, *Nature* **455**, 510 (2008).
  - [33] Unless there are additional constraints to  $\rho$  so that other methods like compressed sensing may apply.
  - [34] For the sake of simplicity here we assume the least square solution gives a physical  $\rho$ , and defer a more careful discussion based on semidefinite programming to Sec. A of [39].
  - [35] J. S. Lundeen, A. Feito, H. Coldenstrodt-Ronge, K. L. Pregnell, C. Silberhorn, T. C. Ralph, J. Eisert, M. B. Plenio, and I. A. Walmsley, *Nat Phys* **5**, 27 (2009).
  - [36] L. Zhang, H. B. Coldenstrodt-Ronge, A. Datta, G. Puentes, J. S. Lundeen, X.-M. Jin, B. J. Smith, M. B.

- Plenio, and I. A. Walmsley, *Nat Photon* **6**, 364 (2012).
- [37] Actually, in some experiments the Wigner function was obtained from  $Q_n^\beta$  [13, 29].
- [38] Z. Leghtas, G. Kirchmair, B. Vlastakis, M. H. Devoret, R. J. Schoelkopf, and M. Mirrahimi, *Phys. Rev. A* **87**, 042315 (2013).
- [39] See supplementary material for details.
- [40] It is note-worthy that examples where tomography requires only one measurement setting is extremely rare.
- [41] This excludes some lines in phase space, lines connecting any pair of points  $(\alpha_i, \alpha_j)$  and the perpendicular bisector of the pair [39].
- [42] R. Bhatia, *Matrix Analysis* (Springer-Verlag, New York, 1997).
- [43] Y. I. Bogdanov, G. Brida, M. Genovese, S. P. Kulik, E. V. Moreva, and A. P. Shurupov, *Phys. Rev. Lett.* **105**, 010404 (2010).
- [44] A. Miranowicz, K. Bartkiewicz, J. Peřina, M. Koashi, N. Imoto, and F. Nori, *Phys. Rev. A* **90**, 062123 (2014).
- [45] A. Miranowicz, i. m. c. K. Özdemir, J. c. v. Bajer, G. Yusa, N. Imoto, Y. Hirayama, and F. Nori, *Phys. Rev. B* **92**, 075312 (2015).
- [46] For even  $m_c$ , the configuration  $\phi_j = \frac{2\pi}{m_c+1}j$ , for  $j = 0, 1, \dots, m_c$  works as well.
- [47] M. Grant and S. Boyd, “CVX: Matlab software for disciplined convex programming, version 2.1,” <http://cvxr.com/cvx> (2014).
- [48] M. Grant and S. Boyd, in *Recent Advances in Learning and Control*, Lecture Notes in Control and Information Sciences, edited by V. Blondel, S. Boyd, and H. Kimura (Springer-Verlag Limited, 2008) pp. 95–110, [http://stanford.edu/~boyd/graph\\_dcp.html](http://stanford.edu/~boyd/graph_dcp.html).
- [49] W. Chen, J. Hu, Y. Duan, B. Braverman, H. Zhang, and V. Vuletić, *Phys. Rev. Lett.* **115**, 250502 (2015).
- [50] A. I. Lvovsky, *Journal of Optics B: Quantum and Semi-classical Optics* **6**, S556 (2004).
-

# Supplemental Materials

## CONTENTS

A. Reconstructing a physical density matrix	2
Enforcing positivity of reconstructed state	2
Enforcing both positivity and trace normalization	2
B. Reconstruction fidelity bound using condition number	3
C. Calculation of a general $Q_n^\beta(\rho)$	4
Special case $p = 1$ & $\alpha_1 = 0$ , general states with a number truncation	4
Special case $m_c = 0$ , cat states	4
D. General dependence of covariance matrix on $\beta$ for general states	5
E. Estimating $\alpha'$ s for cat states	5
F. Informationally incomplete detection regions for cat states	5
G. Fisher Information calculation for cat states	6
H. Informational completeness of a set of $\beta'$ s for general states	7
Typical informational completeness of a set of $(m_c + 1)$ $\beta'$ s	7
Lower bound of the number of settings needed	7
I. Numerical Calculation of the gradient of the condition number	8
Problem Setting	8
Solution with Perturbation Theory	8
Derivative of the Sensing Matrix ( $Qn$ case)	9
Derivative of the Sensing Matrix (Wigner case)	9
J. Optimized Configurations of $\beta'$ s for general states	9
K. Discussion of Full/Half Ring Configurations	10
Multiple full-ring configuration gives lowest condition number	10
Half-ring configuration approximates full-ring well	11
Ring-based schemes for Homodyne tomography	12
L. Comparison of $Q_n$ , Wigner and Homodyne tomography	12
M. Generalized cat states reconstruction	13
Appendix: Proof of Theorem 1	14
Some Preparation	14
Proof of Theorem 1	17
References	22

### A. Reconstructing a physical density matrix

We discuss how one could reconstruct a physical density matrix that best satisfies  $A\vec{\rho} = \vec{b}$ . We start with the simple procedure of enforcing positivity of the reconstructed state and then move on to the more complicated case where both positivity and trace normalization is explicitly enforced.

#### *Enforcing positivity of reconstructed state*

Let  $\vec{\rho}'$  be the least square solution from the noisy measurement record,

$$\vec{\rho}' = (A^\dagger A)^{-1} A^\dagger (\vec{b} + \delta\vec{b}).$$

Generally  $\vec{\rho}'$  may not be positive semidefinite. A natural idea is to truncate the negative eigenvalues of  $\rho'$  (i.e., replace those eigenvalues by 0), in order to obtain a corrected estimate  $\tau$  that is positive semidefinite. That is, if  $\rho'$  has an eigen-decomposition  $\rho' = \sum_i \lambda_i |\psi_i\rangle \langle \psi_i|$ , then we define  $\tau$  to be

$$\tau = \sum_{i: \lambda_i > 0} \lambda_i |\psi_i\rangle \langle \psi_i|.$$

We now show that this procedure can only improve the accuracy of the estimate, in terms of the Frobenius norm (or equivalently, the  $\ell_2$  norm). More precisely, we show that

$$\|\tau - \rho\|_F \leq \|\rho' - \rho\|_F. \quad (\text{S1})$$

First, we show that  $\tau$  is the point in the positive semidefinite cone that lies closest to  $\rho'$  (in the Frobenius norm). That is, we show that for any point  $\zeta \succeq 0$ ,

$$\|\zeta - \rho'\|_F \geq \left[ \sum_{i: \lambda_i < 0} |\langle \psi_i | \zeta | \psi_i \rangle - \lambda_i|^2 \right]^{1/2} \geq \left[ \sum_{i: \lambda_i < 0} |\lambda_i|^2 \right]^{1/2} = \|\tau - \rho'\|_F. \quad (\text{S2})$$

Then, suppose (for contradiction) that Eq. (S1) does not hold, which implies that  $\|\tau - \rho\|_F > \|\rho' - \rho\|_F$ . Now consider the triangle whose vertices are  $\rho$ ,  $\rho'$  and  $\tau$ . Let  $\theta \in [0, \pi]$  be the angle at the vertex  $\tau$ . Using the Law of Cosines, we have that

$$\cos \theta = \frac{\|\rho' - \tau\|_F^2 - \|\rho - \rho'\|_F^2 + \|\rho - \tau\|_F^2}{2 \|\rho' - \tau\|_F \|\rho - \tau\|_F} > 0.$$

This implies that  $0 \leq \theta < \pi/2$ , i.e., the angle at  $\tau$  is less than 90 degrees.

Hence, there exists a point  $\zeta$  that is a convex combination of  $\tau$  and  $\rho$  such that  $\|\zeta - \rho'\|_F < \|\tau - \rho'\|_F$ . Moreover, since  $\rho \succeq 0$  and  $\tau \succeq 0$ , it follows that  $\zeta \succeq 0$ . This contradicts Eq. (S2). Therefore, we conclude that Eq. (S1) must hold.

#### *Enforcing both positivity and trace normalization*

If one wants to enforce both positive semidefiniteness and trace normalization, one needs to solve the semidefinite program (SDP)

$$\begin{aligned} & \text{minimize } \|\sigma - \rho'\|_F \\ & \text{subject to } \sigma \succeq 0, \text{ tr } \sigma = 1. \end{aligned}$$

Note that SDP can be solved efficiently using the Matlab package CVX [47, 48].

Denoting the solution of this SDP as  $\tau$ , we still have

$$\|\zeta - \rho'\|_F \geq \|\tau - \rho'\|_F$$

where now  $\zeta \succeq 0$  and  $\text{tr } \zeta = 1$ . And the triangle argument still goes through since the set  $\{\rho | \rho \succeq 0, \text{ tr } \rho = 1\}$  is also convex. Eventually, the fact below still holds

$$\|\tau - \rho\|_F \leq \|\rho' - \rho\|_F.$$



### B. Reconstruction fidelity bound using condition number

We derive a lower bound on the fidelity of reconstruction in terms of condition number here. We will first find an upper bound for the trace distance of the reconstructed state to the true state, and then get the fidelity bound using the relation between fidelity and trace distance  $D(\rho, \sigma)$ ,

$$F(\rho, \sigma) \geq 1 - D(\rho, \sigma)$$

where  $D(\rho, \sigma) = \frac{1}{2} \|\rho - \sigma\|_{\text{tr}}$ .

Let  $\vec{\rho}$  be the true state and  $\vec{\rho}'$  be the least square solution from the noisy measurement record,

$$\begin{aligned}\vec{\rho} &= (A^\dagger A)^{-1} A^\dagger \vec{b}, \\ \vec{\rho}' &= (A^\dagger A)^{-1} A^\dagger (\vec{b} + \delta \vec{b}),\end{aligned}$$

and define  $\delta \vec{\rho} \equiv \vec{\rho} - \vec{\rho}' = \tilde{A}^{-1} \delta \vec{b} = (A^\dagger A)^{-1} A^\dagger \delta \vec{b}$ .

Following the main text we use the 2-norm for vectors  $\vec{\rho}$  to define the condition number, then

$$\left( \frac{\|\delta \vec{\rho}\|_2}{\|\vec{\rho}\|_2} \right) / \left( \frac{\|\delta \vec{b}\|_2}{\|\vec{b}\|_2} \right) \leq \kappa(A).$$

Since the Frobenius norm of a matrix is the same as the 2-norm of it when arranged as a vector,

$$\|\rho\|_F = \|\vec{\rho}\|_2 \leq \kappa(A) \|\rho\|_F \frac{\|\delta \vec{b}\|_2}{\|\vec{b}\|_2}.$$

Let  $\tau$  be the semi-positive and trace normalized density matrix that best satisfies the noisy measurement record  $A\tau = \vec{b} + \delta \vec{b}$ , obtained as described in the previous section. We have

$$\|\rho - \tau\|_F \leq \|\rho - \rho'\|_F = \|\delta \rho\|_F \leq \kappa(A) \|\rho\|_F \frac{\|\delta \vec{b}\|_2}{\|\vec{b}\|_2},$$

where the first inequality uses Eq. (S1). The above bound is useful since it upper bounds the distance (in terms of Frobenius norm) between the reconstructed state and the true state.

Using the relation between the trace norm and Frobenius norm

$$\|M\|_{\text{tr}} \leq \sqrt{r} \|M\|_F$$

we find

$$D(\rho, \tau) \leq \frac{1}{2} \sqrt{r} \|\rho - \tau\|_F \leq \frac{1}{2} \sqrt{r} \kappa(A) \|\rho\|_F \frac{\|\delta \vec{b}\|_2}{\|\vec{b}\|_2}$$

and

$$F(\rho, \tau) \geq 1 - D(\rho, \tau) \geq 1 - \frac{1}{2} \sqrt{r} \kappa(A) \|\rho\|_F \frac{\|\delta \vec{b}\|_2}{\|\vec{b}\|_2}. \quad (\text{S3})$$

In practice we have an estimate for the measurement noise  $\epsilon \sim \frac{\|\delta \vec{b}\|_2}{\|\vec{b}\|_2}$  and the truncation dimension  $d$  upperbounds the rank  $r$  of  $\delta \rho$ . Since  $\rho$  is unknown we replace it with the reconstructed  $\tau$ . In this way an approximate bound on the fidelity can be calculated,  $F(\rho, \tau) \gtrsim 1 - \frac{1}{2} \epsilon \sqrt{d} \kappa(A) \|\tau\|_F$ .

We now see that minimizing the condition number  $\kappa(A)$  is in fact maximizing a lower bound of the reconstruction fidelity.

### C. Calculation of a general $Q_n^\beta(\rho)$

We derive the expression of  $Q_n^\beta(\rho)$  for “patch states”  $\rho = \sum_{i,j,m_1,m_2} \rho_{i,m_1;j,m_2} |\alpha_i, m_1\rangle \langle \alpha_j, m_2|$ , where  $|\alpha_i, m_j\rangle \equiv D(\alpha_i) |m_j\rangle$ .

$$Q_n^{(\beta)}(\rho) \equiv \langle \beta, n | \rho | \beta, n \rangle = \sum_{i,j,m_1,m_2} \rho_{i,m_1;j,m_2} Q_n^{(\beta)}(|\alpha_i, m_1\rangle \langle \alpha_j, m_2|),$$

where  $m_1, m_2$  range from 0 to  $m_c$  and

$$Q_n^{(\beta)}(|\alpha_i, m_1\rangle \langle \alpha_j, m_2|) = e^{i\theta(\alpha_i, \beta) - i\theta(\alpha_j, \beta)} \langle n | D(\alpha_i - \beta) | m_1 \rangle \langle m_2 | D(\beta - \alpha_j) | n \rangle,$$

where we have used

$$D(\alpha)D(\beta) = e^{(\alpha\beta^* - \alpha^*\beta)/2} D(\alpha + \beta) \equiv e^{i\theta(\alpha, \beta)} D(\alpha + \beta).$$

Using the expressions for matrix elements of the displacement operator,

$$\begin{aligned} \langle m | D(\alpha) | n \rangle &= \sqrt{\frac{n!}{m!}} \alpha^{m-n} e^{-\frac{1}{2}|\alpha|^2} \mathcal{L}_n^{m-n}(|\alpha|^2) \\ &= (-1)^{n-m} \sqrt{\frac{m!}{n!}} (\alpha^{n-m})^* e^{-\frac{1}{2}|\alpha|^2} \mathcal{L}_m^{n-m}(|\alpha|^2), \end{aligned}$$

where  $\mathcal{L}_m^{n-m}(x)$  is the associated Laguerre polynomial.

We obtain after some work

$$\begin{aligned} &Q_n^{(\beta)}(|\alpha_i, m_1\rangle \langle \alpha_j, m_2|) \\ &= e^{i\theta(\alpha_i, \beta) - i\theta(\alpha_j, \beta)} e^{-\frac{1}{2}(|\alpha_i - \beta| - |\alpha_j - \beta|)^2} \times \frac{1}{n!} [(\alpha_i - \beta)(\alpha_j - \beta)^*]^n e^{-|\alpha_i - \beta| \cdot |\alpha_j - \beta|} \\ &\times \frac{\sqrt{m_1!}}{(\alpha_i - \beta)^{m_1}} \mathcal{L}_{m_1}^{n-m_1}(|\alpha_i - \beta|^2) \frac{\sqrt{m_2!}}{[(\alpha_j - \beta)^{m_2}]^*} \mathcal{L}_{m_2}^{n-m_2}(|\alpha_j - \beta|^2). \end{aligned} \quad (\text{S4})$$

Notice that **(a)** the part

$$\frac{1}{n!} [(\alpha_i - \beta)(\alpha_j - \beta)^*]^n e^{-|\alpha_i - \beta| \cdot |\alpha_j - \beta|} = \frac{1}{n!} [|\alpha_i - \beta| \cdot |\alpha_j - \beta| e^{i\phi}]^n e^{-|\alpha_i - \beta| \cdot |\alpha_j - \beta|}$$

is a complex Poissonian distribution where  $\phi$  is the angle between vectors  $(\alpha_i - \beta)$  and  $(\alpha_j - \beta)$ ; **(b)** The signal is damped by the factor  $e^{-\frac{1}{2}(|\alpha_i - \beta| - |\alpha_j - \beta|)^2}$ , i.e. when the detection position  $\beta$  is much closer to  $\alpha_i$  than to  $\alpha_j$ , the signal vanishes. The contour lines of such a damping factor are hyperbolas whose foci are  $\alpha_i$  and  $\alpha_j$ ; **(c)** The associated Laguerre polynomials  $\mathcal{L}_m^{n-m}(x)$  are of order  $m$  in the variable  $x$ , and also of order  $m$  in  $(n - m)$ .

*Special case  $p = 1$  &  $\alpha_1 = 0$ , general states with a number truncation*

Let us now look at the case where there is only one patch ( $p = 1$ ), without loss of generality located at the origin ( $\alpha_1 = 0$ ),  $\rho = \sum_{m_1, m_2=0}^{m_c} \rho_{m_1 m_2} |m_1\rangle \langle m_2|$ . We have

$$Q_n^\beta(\rho) = \left( e^{-|\beta|^2} \frac{1}{n!} |\beta|^{2n} \right) \sum_{m_1, m_2=0}^{m_c} \rho_{m_1 m_2} \times \frac{\sqrt{m_1! m_2!}}{(-\beta)^{m_1} (-\beta^*)^{m_2}} \mathcal{L}_{m_1}^{n-m_1}(|\beta|^2) \mathcal{L}_{m_2}^{n-m_2}(|\beta|^2).$$

*Special case  $m_c = 0$ , cat states*

Let us look at a simplified case where each displaced Fock state has photon cutoff  $m_c = 0$ , i.e. we have a superposition of coherent states,  $\rho = \sum_{i,j=1}^p \rho_{ij} |\alpha_i\rangle \langle \alpha_j|$ . In this case

$$Q_n^\beta(\rho) = \sum_{i,j=0}^p \rho_{ij} Q_n^\beta(|\alpha_i\rangle \langle \alpha_j|) = \sum_{i,j=0}^p \tilde{\rho}_{ij} \frac{1}{n!} [d_i d_j e^{i\phi_{ij}}]^n \quad (\text{S5})$$

where we defined  $\tilde{\rho}_{ij} \equiv e^{i\theta(\beta, \alpha_i, \alpha_j)} e^{-\frac{1}{2}(d_i - d_j)^2} e^{-d_i d_j} \rho_{ij}$ ,  $d_i \equiv |\alpha_i - \beta|$ , and  $\phi_{ij} \equiv \arg(\alpha_i - \beta) - \arg(\alpha_j - \beta)$ .

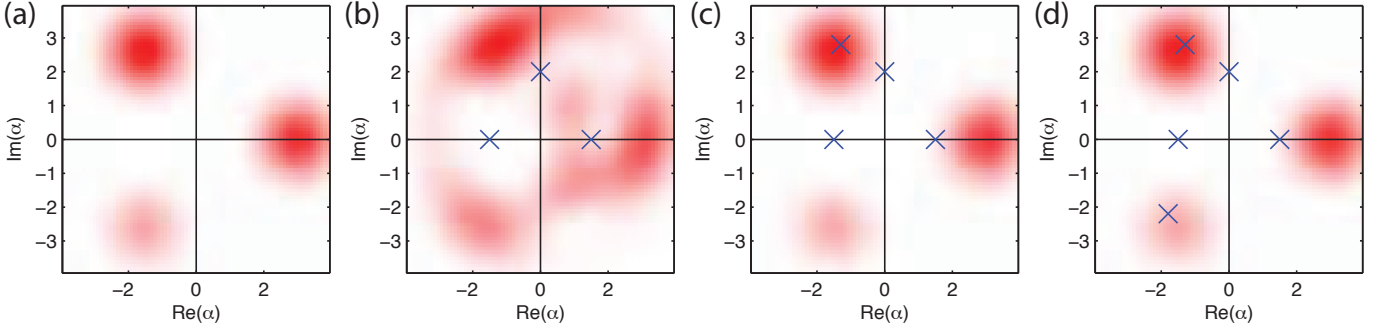


Figure S1. Procedure of estimating the  $\alpha_i$  via Husimi Q function. (a) shows the true Q function of the state; (b) shows the estimated Q function via iMLE after measuring  $Q_n^\beta(\rho)$  at three  $\beta'$ s shown as the crosses; (c)/(d) are estimations after measuring at four/five  $\beta'$ s. Apparently estimate in (c) already converges to the true Q function shown in (a).

#### D. General dependence of covariance matrix on $\beta$ for general states

Using

$$\begin{aligned} A_{(n,\beta),(m_1,m_2)} &= \text{tr} [D(\beta) |n\rangle \langle n| D(-\beta) |m_1\rangle \langle m_2|] \\ &= e^{-|\beta|^2} \times \frac{1}{n!} |\beta|^{2n} \times \frac{\sqrt{m_1!}}{(-\beta)^{m_1}} \mathcal{L}_{m_1}^{n-m_1}(|\beta|^2) \frac{\sqrt{m_2!}}{[(-\beta)^{m_2}]^*} \mathcal{L}_{m_2}^{n-m_2}(|\beta|^2), \end{aligned} \quad (\text{S6})$$

we see that

$$A_{(n,\beta),(m_1,m_2)} \propto \beta^{m_2-m_1} g_{m_1 m_2}(|\beta|).$$

Therefore

$$\begin{aligned} C_{(m_1 m_2),(n_1 n_2)} &= \sum_{n,j} A_{(n,\beta_j),(m_1,m_2)}^* A_{(n,\beta_j),(n_1,n_2)} \\ &\propto \sum_{\beta_j} \beta_j^{m_1-m_2-n_1+n_2} f_{m_1,m_2,n_1,n_2}(|\beta_j|). \end{aligned}$$

#### E. Estimating $\alpha'$ s for cat states

Measuring  $Q_n^\beta(\rho)$  for around 3 different  $\beta'$ s, we can estimate the values of  $\alpha'$ s using the iterative maximum likelihood estimation (iMLE) technique [50]. Because  $Q_n^\beta(\rho)$  provides the information about the distances between  $\alpha_i$  and  $\beta$ , we expect that measuring  $Q_n^\beta(\rho)$  at 3 different  $\beta'$ s can completely fix all  $\alpha_i$ . Depending on the result one can additionally measure at one or two  $\beta'$ s, preferably at the current estimated  $\alpha'_i$ s, to increase the certainty of estimate. We show one example in Fig. S1, which shows that four  $\beta'$ s are enough to accurately estimate the  $\alpha'$ s.

#### F. Informationally incomplete detection regions for cat states

From Eq. (S5),

$$Q_n^\beta(\rho) = \sum_{i,j=0}^p \tilde{\rho}_{ij} \frac{1}{n!} [d_i d_j e^{i\phi_{ij}}]^n,$$

we see that under the following conditions all the  $d_i d_j e^{i\phi_{ij}}$  are distinct (i)  $d_i \neq d_j$ , other wise the columns corresponding to  $\tilde{\rho}_{ii}$  and  $\tilde{\rho}_{jj}$  would be identical;; (ii)  $\phi_{ij} \neq 0, \pi$ , otherwise the columns  $\tilde{\rho}_{ij}$  and  $\tilde{\rho}_{ji}$  would be identical; (iii)  $d_i d_j \neq d_k d_l$  or  $\phi_{ij} \neq \phi_{kl}$  where all of  $i, j, k, l$  are assumed to be distinct. These requirements have clear geometric interpretations: (i)  $\beta$  does not lie on the perpendicular bisector of the line segment  $\alpha_i \alpha_j$ ; (ii)  $\beta, \alpha_i, \alpha_j$  are not collinear; (iii) triangles

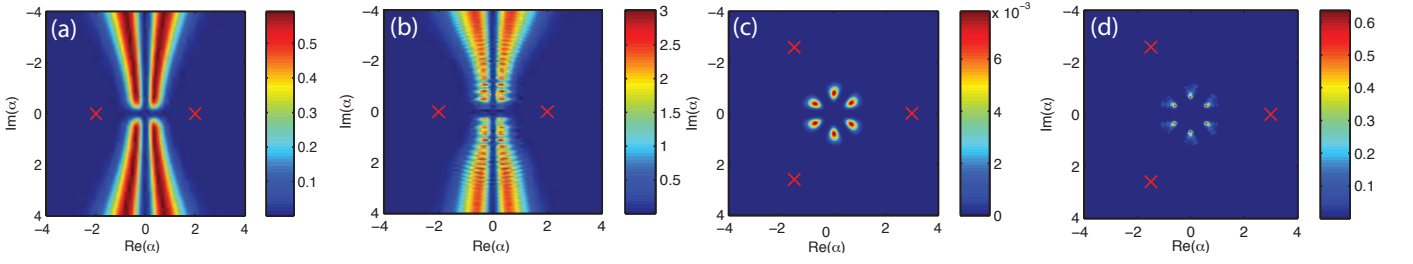


Figure S2. Determinant of the Fisher information  $\mathcal{I}(\vec{\rho})$  as a function of  $\beta$  for four different states. (a) Two-component maximally mixed cat state,  $\rho_{ij} \propto \delta_{ij}$ . In other words, the Bloch vector is 0; (b) A two component cat state, with Bloch vector  $0.9 \cdot (1, 1, 0)/\sqrt{2}$ ; (c) Three-component maximally mixed cat state,  $\rho_{ij} \propto \delta_{ij}$ ; (d) A mixture  $\rho = (1 - \lambda)I/3 + \lambda|\psi\rangle\langle\psi|$  where  $I$  is the identity and  $|\psi\rangle = (1, 1, 1)^\dagger/\sqrt{3}$ . The shape of the good detection region for maximally mixed states are very similar to that predicted by the condition number while for higher purity states additional “interference fringes” appear. The worst of Fisher information over all true states should be that of the maximally mixed states, whose results agree well with that given by condition number.

formed by  $(\beta, \alpha_i, \alpha_j)$  and  $(\beta, \alpha_k, \alpha_l)$  do not have the same area or the angles subtended by  $\overline{\alpha_i \alpha_j}$  and  $\overline{\alpha_k \alpha_l}$  from  $\beta$  are different. There is in fact one extra requirement, due to the factor  $e^{-\frac{1}{2}(d_i - d_j)^2}$  in  $Q_n^\beta(|\alpha_i\rangle\langle\alpha_j|)$ . When  $d_i \ll d_j$  or  $d_i \gg d_j$ ,  $\rho_{ij}$  gets exponentially suppressed and almost vanishes from the sensing equation, just like the case with the conventional Husimi Q function. So we add one requirement (iv)  $\beta$  does not lie far away from the bisector of  $\alpha_i \alpha_j$  in the sense that  $e^{-\frac{1}{2}(d_i - d_j)^2}$  is not too small. Requirement (iv) is closely related to the error robustness.

### G. Fisher Information calculation for cat states

For the state

$$\rho = \sum_{i,j=1}^p \rho_{ij} |\alpha_i\rangle\langle\alpha_j|$$

with known  $\alpha_i$ , the parameters to be estimated are  $\rho_{ij}$ . For convenience we arrange the  $p^2$  numbers as a vector  $\vec{\rho}$ . For a certain measurement position  $\beta$ , we can get a distribution

$$f(n) \equiv Q_n^\beta(\rho).$$

According to the definition, the Fisher information matrix is

$$\begin{aligned} \mathcal{I}(\vec{\rho}) &= \mathbb{E}_{\vec{\rho}} \left[ \left( \frac{\partial}{\partial \vec{\rho}} \log f(n) \right) \cdot \left( \frac{\partial}{\partial \vec{\rho}} \log f(n) \right)^\dagger \right] \\ &= \sum_{n=0}^{\infty} \frac{1}{f(n)} \left( \frac{\partial}{\partial \vec{\rho}} f(n) \right) \cdot \left( \frac{\partial}{\partial \vec{\rho}} f(n) \right)^\dagger, \end{aligned}$$

where

$$\frac{\partial f}{\partial \rho_{ij}} = Q_n^\beta(|\alpha_i\rangle\langle\alpha_j|).$$

Notice that  $\mathcal{I}(\vec{\rho})$  is a matrix-valued function depending on the true state specified by  $\vec{\rho}$ . We use the determinant of  $\mathcal{I}(\vec{\rho})$  as a one-parameter measure of the information contained in the measurement  $Q_n^\beta(\rho)$  and plot  $\det \mathcal{I}(\vec{\rho})$  as a function of  $\beta$  for a few different  $\vec{\rho}$ , see Fig. S2.

## H. Informational completeness of a set of $\beta'$ s for general states

*Typical informational completeness of a set of  $(m_c + 1)$   $\beta'$ s*

The full  $Q_n^\beta$  can be written as a polynomial of  $n$

$$\begin{aligned} Q_n^\beta(\rho) &= Q_n^\beta \left( \sum_{m_1, m_2}^{m_c} \rho_{m_1 m_2} |m_1\rangle \langle m_2| \right) \\ &= n^{2m_c} \cdot c_{2m_c}^\beta(\rho_{m_c m_c}) \\ &\quad + n^{2m_c-1} \cdot c_{2m_c-1}^\beta(\rho_{m_c m_c}, \rho_{m_c, m_c-1}, \rho_{m_c-1, m_c}) \\ &\quad + \dots + n^k \cdot c_k^\beta(\{\rho_{m_1 m_2}\}_{m_1+m_2 \geq k}) + \dots \\ &\quad + n^1 \cdot c_1^\beta(\{\rho_{m_1 m_2}\}_{m_1+m_2 \geq 1}) + n^0 \cdot c_0^\beta(\{\rho_{m_1 m_2}\}), \end{aligned}$$

where we used  $c_k^\beta(\{\bullet\})$  to indicate the dependence of coefficients on elements of  $\rho$ . From the measured  $Q_n^{\beta_1}$  we can in principle fit a polynomial and get all the coefficients  $Q_n^{\beta_1}(\rho) = \sum_{k=0}^{2m_c} n^k \cdot \tilde{c}_k^{\beta_1}$ . Each  $c_k^{\beta_1}$  gives us an independent equation about variables  $\{\rho_{m_1 m_2}\}_{m_1+m_2 \geq k}$ . The dependence of  $c_k^\beta$  on  $\rho_{m_1 m_2}$  is shown below (omitting  $\beta$  superscript on  $c_k$ ):

$$\begin{aligned} c_{2m_c} &\sim \rho_{m_c, m_c} \\ c_{2m_c-1} &\sim \rho_{m_c, m_c}, \rho_{m_c-1, m_c}, \rho_{m_c, m_c-1} \\ &\vdots \\ c_{m_c} &\sim \rho_{0, m_c}, \rho_{1, m_c-1}, \dots, \rho_{m_c, 0} \text{ and all variables that appear above} \\ c_{m_c+1} &\sim m_c \text{ new terms and all variables that appear above} \\ &\vdots \\ c_0 &\sim \text{all variables above} \end{aligned}$$

where by “variables” we mean elements of the density matrix,  $\rho_{m_1, m_2}$ . This argument is similar to that of [9]. Assume we have measured at  $\beta_1, \beta_2, \dots, \beta_{m_c+1}$ . We then have  $(m_c + 1)$  equations for each  $c_k$ . To find  $\rho_{m_c, m_c}$  we only need  $c_k^{\beta_1}$  and the rest measurements do not offer new information. After figuring out  $\rho_{m_c, m_c}$ ,  $c_{2m_c-1}$  now has only two unknown variables and we only need  $c_k^{\beta_1}$  and  $c_k^{\beta_2}$  to figure them out. We can continue in this way and solve all the variables that appear in  $c_{2m_c}, c_{2m_c-1}, \dots$ , down to  $c_0$  because when solving each of them all the variables that appear before are unknown and they contain less than or equal to  $m_c + 1$  unknowns.

### *Lower bound of the number of settings needed*

Assume the excitation number cutoff for the unknown state is  $m_c$ . The first measurement at  $\beta_1$  gives  $2m_c + 1$  independent equations and each successive measurement setting gives at most one less independent equations. Assume the number of settings is  $N_\beta$ , where  $N_\beta \leq 2m_c + 1$ . The total number of independent equations is at most

$$(2m_c + 1) + (2m_c) + (2m_c - 1) + \dots + (2m_c - N_\beta + 2) = N_\beta(4m_c - N_\beta + 3)/2.$$

The total number of unknown variables is  $(m_c + 1)^2$ . Letting

$$N_\beta(4m_c - N_\beta + 3)/2 \geq (m_c + 1)^2$$

we obtain

$$\frac{1}{2} \left[ 3 + 4m_c - \sqrt{8m_c^2 + 8m_c + 1} \right] \leq N_\beta \leq \frac{1}{2} \left[ 3 + 4m_c + \sqrt{8m_c^2 + 8m_c + 1} \right].$$



The constraint  $N_\beta \leq \frac{1}{2} \left[ 3 + 4m_c + \sqrt{8m_c^2 + 8m_c + 1} \right]$  is weaker than  $N_\beta \leq 2m_c + 1$  and we can ignore it. The remaining constraint is simplified to

$$\begin{aligned} N_\beta &\geq \frac{1}{2} \left[ 3 + 4m_c - \sqrt{8m_c^2 + 8m_c + 1} \right] \\ &= \frac{3}{2} + m_c \left[ 2 - \sqrt{2 + \frac{1}{4} \left( \frac{1}{m_c} + \frac{1}{m_c^2} \right)} \right]. \end{aligned}$$

In the large  $m_c$  limit the lower bound becomes simply

$$N_\beta \gtrsim \frac{3}{2} + 0.59m_c.$$

## I. Numerical Calculation of the gradient of the condition number

We show how to calculate the gradient of a matrix's condition number using perturbation theory, in the context of the state tomography problem.

### *Problem Setting*

We want to construct an optimal sensing matrix  $A(\beta_i)$ , parameterized by a few continuous variables,  $\beta_i$ , such that state tomography using the sensing map  $A \cdot \rho = b$  has the optimal error robustness, i.e. the condition number  $\kappa(A)$  is minimal.

It is obvious how to evaluate  $\kappa(A)$  given the  $\beta_i$ . It will be very helpful for the optimization if we also have direct access to the gradients  $\partial_{\beta_i} \kappa(A)$ .

### *Solution with Perturbation Theory*

Let us perturb matrix  $A$  by changing  $\beta_i$  infinitesimally,

$$\begin{aligned} A(\beta_i + \delta\beta_i) &= A + \delta\beta_i (\partial_{\beta_i} A) \\ &\equiv A + \delta\beta_i B_i. \end{aligned}$$

Note that we are changing only one  $\beta_i$  so there's no summation over  $i$  here. We try to find  $\partial_{\beta_i} \kappa(A)$ . For convenience we choose to work with the Hermitian matrix  $\tilde{A} \equiv A^\dagger A$  whose condition number is  $\kappa(\tilde{A}) = \kappa(A^\dagger A) = \kappa(A)^2$ .

$$\begin{aligned} \partial_{\beta_i} \kappa(\tilde{A}) &= \partial_{\beta_i} \frac{\epsilon_{\max}(\tilde{A})}{\epsilon_{\min}(\tilde{A})} \\ &= \frac{\partial_{\beta_i} \epsilon_{\max}(\tilde{A}) \epsilon_{\min}(\tilde{A}) - \epsilon_{\max}(\tilde{A}) \partial_{\beta_i} \epsilon_{\min}(\tilde{A})}{\epsilon_{\min}(\tilde{A})^2}, \end{aligned} \tag{S7}$$

where  $\epsilon_{\max}/\epsilon_{\min}$  are the largest/smallest eigenvalues of  $\tilde{A}$ . Now the problem reduces to calculate the gradient of the eigenvalues of  $\tilde{A}$  with respect to  $\beta_i$ .

It is well known in quantum mechanics that the first order perturbation to the energy of the  $k$ -th eigenstate is

$$\delta\epsilon_k = \langle \psi_k | \delta H | \psi_k \rangle$$

where  $|\psi_k\rangle$  is the  $k$ -th eigenstate of the unperturbed Hamiltonian  $H$  and  $\delta H$  is a small perturbation.

In our case,

$$\tilde{A}' = \tilde{A} + \delta\beta_i (B_i^\dagger A + A^\dagger B_i) + O(\delta\beta^2),$$

so

$$\partial_{\beta_i} \epsilon_k(\tilde{A}) = v_k^\dagger (B_i^\dagger A + A^\dagger B_i) v_k \tag{S8}$$

where  $v_k$  is the  $k$ -th eigenvector of  $\tilde{A}$ . Using the above expression Eq (S8) for the smallest and largest eigenvalues, we have all the required quantities to determine the gradient of the condition number following Eq (S7).

*Derivative of the Sensing Matrix (Qn case)*

We now apply the method developed previously to the state tomography problem using photon number counting measurements (generalized Q function).

Using

$$\begin{aligned} D(\beta) &= e^{-\frac{1}{2}|\beta|^2} e^{+\beta a^\dagger} e^{-\beta^* a}, \\ D(\beta) &= e^{+\frac{1}{2}|\beta|^2} e^{-\beta^* a} e^{+\beta a^\dagger}, \end{aligned}$$

we can verify that

$$\begin{aligned} \partial_\beta D(\beta) &= (a^\dagger - \frac{1}{2}\beta^*) D(\beta), \\ \partial_{\beta^*} D(\beta) &= (\frac{1}{2}\beta - a) D(\beta), \\ \partial_\beta D^\dagger(\beta) &= D^\dagger(\beta) (\frac{1}{2}\beta^* - a^\dagger), \\ \partial_{\beta^*} D^\dagger(\beta) &= D^\dagger(\beta) (-\frac{1}{2}\beta + a). \end{aligned}$$

After some calculation we obtain that

$$\partial_\beta [D(\beta) |n\rangle \langle n| D^\dagger(\beta)] = [a^\dagger, D(\beta) |n\rangle \langle n| D^\dagger(\beta)],$$

and

$$\partial_{\beta^*} [D(\beta) |n\rangle \langle n| D^\dagger(\beta)] = \{\partial_\beta [D(\beta) |n\rangle \langle n| D^\dagger(\beta)]\}^\dagger.$$

If  $\rho$  is a general state  $\rho = \sum_{m_1, m_2=0}^{m_c} \rho_{m_1 m_2} |m_1\rangle \langle m_2|$ , using Eq. (S6) we get

$$\begin{aligned} \partial_\beta A_{(n, \beta); (m_1, m_2)} &= \sqrt{m_2} Q_n^\beta (|m_1\rangle \langle m_2 - 1|) - \sqrt{m_1 + 1} Q_n^\beta (|m_1 + 1\rangle \langle m_2|), \\ \partial_{\beta^*} A_{(n, \beta); (m_1, m_2)} &= -\sqrt{m_2 + 1} Q_n^\beta (|m_1\rangle \langle m_2 + 1|) + \sqrt{m_1} Q_n^\beta (|m_1 - 1\rangle \langle m_2|). \end{aligned}$$

In the exact same manner, the sensing matrix and its derivatives can be found for cat states  $\rho = \sum_{i,j=1}^p \rho_{ij} |\alpha_i\rangle \langle \alpha_j|$ ,

$$A_{(n, \beta); (i, j)} = \langle 0| D(-\alpha_j) D(\beta) |n\rangle \langle n| D(-\beta) D(\alpha_i) |0\rangle,$$

and

$$\partial_\beta A_{(n, \beta); (i, j)} = \langle \alpha_j| [a^\dagger, D(\beta) |n\rangle \langle n| D^\dagger(\beta)] |\alpha_i\rangle$$

*Derivative of the Sensing Matrix (Wigner case)*

The Wigner case is simpler to calculate. The row of the sensing matrix corresponding to measurement at  $\beta$  has the form

$$\begin{aligned} W_{\beta; (m_1 m_2)} &= W^\beta (|m_1\rangle \langle m_2|) \\ &= (-1)^{m_1} \langle m_2| D(2\beta) |m_1\rangle \end{aligned}$$

and its derivative can be shown to be

$$\begin{aligned} \partial_\beta W_{\beta; (m_1 m_2)} &= 2(-1)^{m_1} [\sqrt{m_2} \langle m_2 - 1| D(2\beta) |m_1\rangle - \beta^* \langle m_2| D(2\beta) |m_1\rangle], \\ \partial_{\beta^*} W_{\beta; (m_1 m_2)} &= 2(-1)^{m_1} [\beta \langle m_2| D(2\beta) |m_1\rangle - \sqrt{m_2 + 1} \langle m_2 + 1| D(2\beta) |m_1\rangle]. \end{aligned}$$

The rest of calculation follows the case for  $Q_n$  measurements.

## J. Optimized Configurations of $\beta'$ s for general states

We show some examples of optimized configurations of  $\beta'$ s for  $Q_n$ /Wigner measurements in Fig S3. The optimal configuration of  $\beta'$ s for  $Q_n$  measurements typically have the half-ring configuration, in agreement with our theoretical argument in the next section.

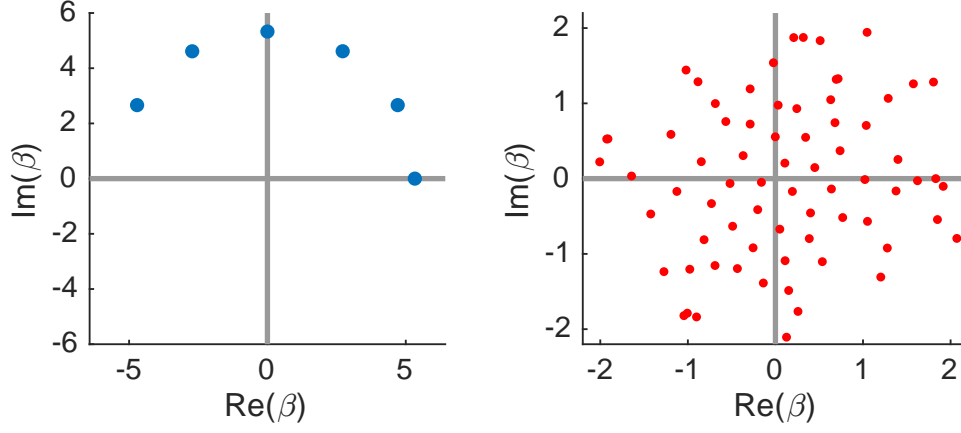


Figure S3. Optimized configurations of  $\beta'$ s for  $Q_n$ /Wigner measurements for a target state with  $m_c = 5$ . For  $Q_n$  measurements 6  $\beta'$ s are needed while for Wigner measurements 72  $\beta'$ s are needed.

### K. Discussion of Full/Half Ring Configurations

*Multiple full-ring configuration gives lowest condition number*

Let us prove that the multiple full-ring configuration (MFRC) can give the minimal condition number if we do not limit the number of measurement settings. Note that we allow rings having different radii to consist of different numbers (at least  $(m_c + 1)$  or  $(m_c + 2)$  depending on whether  $m_c$  is even or odd) of points equally spaced. Our argument consists of two main steps. (a) Given a candidate set for optimal configuration  $\{\beta_i\}$  where  $|\beta_i| = r$ , we can always decrease CN by rearranging/adding  $\beta'$ s such that the configuration becomes FRC. (b) For any given candidate set for optimal configuration  $\{\beta_i\}$ , we can always decrease the condition number by rearranging/adding  $\beta'$ s such that the configuration becomes a collection of FRC, i.e. MFRC.

*Step (a).* Let us partition the indices  $(m_1, m_2)$  into groups according to  $k \equiv m_1 - m_2$ . The group with  $k = \pm m_c$  clearly has only one element  $(m_c, 0)$  and the group with a general  $k$  has  $(m_c - |k| + 1)$  elements. Using such a partition, we divide the covariance matrix into blocks  $C = [C_{k_1 k_2}]$ . Since the covariance matrix has elements  $C_{(m_1 m_2), (n_1 n_2)} = \sum_j \beta_j^{m_1 - m_2 - n_1 + n_2} f_{m_1, m_2, n_1, n_2}(|\beta_j|)$ , each element in block  $C_{k_1 k_2}$  is a linear combination of  $\beta_j^{k_1 - k_2}$ . In particular, the diagonal blocks  $C_{kk}$  does not depend on the complex angles of the  $\beta'$ s. If all the  $\beta'$ s have the same magnitude, every element in block  $C_{k_1 k_2}$  is proportional to  $\sum_j e^{-i(k_1 - k_2)\phi_j}$  where  $\phi_j$  is the complex angle of  $\beta_j$ . It is possible to make  $\sum_j e^{i(k_1 - k_2)\phi_j} = \delta_{k_1 k_2}$  for all  $k_1, k_2$  and thus wipe out all the off-diagonal blocks if the number of  $\beta'$ s  $N_\beta$  is no smaller than  $(2m_c + 1)$  and  $\phi_j$  are equally spaced from 0 and  $2\pi$ . If  $N_\beta < 2m_c + 1$ , we simply add  $\beta'$ s (we are not concerned with the number of measurements at the moment). For the diagonal blocks, adding  $\beta'$ s gives them a global multiplicative factor  $\frac{2m_c + 1 - N_\beta}{N_\beta}$ , which can be factored out since it does not affect the CN. Mathematically wiping out all the off-diagonal blocks is called “pinching” and is formally described as

$$C \mapsto \tilde{C} = \sum_k P_k C P_k$$

where  $P_k$  is the projector to the subspace corresponding to the block  $C_{kk}$ . It is known that the eigenvalues of  $\tilde{C}$  are majorized by those of  $C$  (see page 50 of [42]), i.e.  $\sum_{i=1}^k \lambda_i^\downarrow(\tilde{C}) \leq \sum_{i=1}^k \lambda_i^\downarrow(C)$  for  $k = 1, 2, \dots, D$  and  $\sum_{i=1}^D \lambda_i^\downarrow(\tilde{C}) = \sum_{i=1}^D \lambda_i^\downarrow(C)$ , where  $\lambda_i^\downarrow$  are the eigenvalues in descending order and  $D$  is the dimension of  $C$  and  $\tilde{C}$ . This implies that  $\kappa(\tilde{C}) \leq \kappa(C)$ . This fact can also be understood in the language of quantum mechanics. View  $\tilde{C}$  as a block-diagonal Hamiltonian  $H_0$  and  $C - \tilde{C}$  as a perturbation  $H_1$  coupling different subspaces of  $H_0$ . It is well known that energy levels repel each other when coupled to each other. So the highest of energy level gets higher and the lowest gets lower, with their ratio being increased. This means that among the sets of  $\beta'$ s with the same magnitude, FRC can give the optimal CN.

*Step (b).* Assume the candidate set now contains  $\beta'$ s with different magnitudes. Let  $n_\mu$  of the  $\beta'$ s have magnitude  $r_\mu$  and they form a subset  $B_\mu$ . Using the results of step (a) we can add/rearrange the  $\beta'$ s such that the off-diagonal blocks are all wiped out. However such an operation is not guaranteed to be a pinching since now there may be a

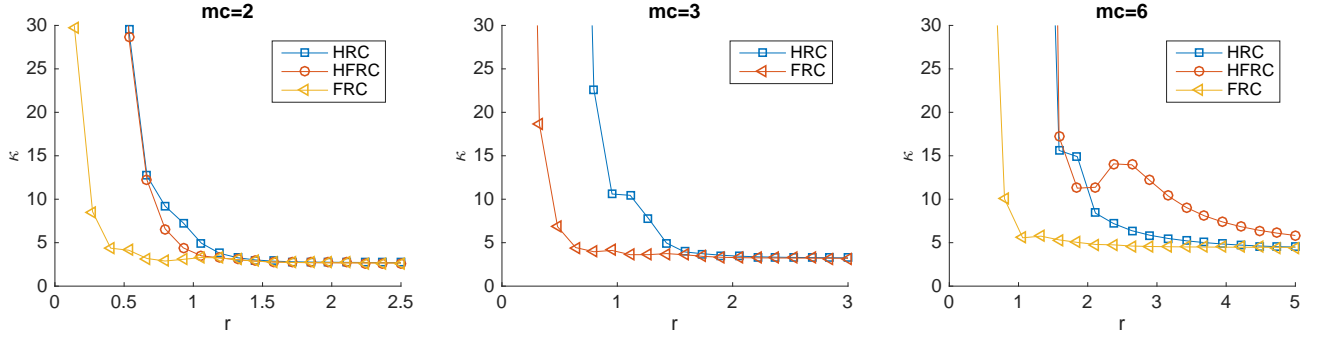


Figure S4. Comparison condition number as a function of ring radius for different configurations. HRC: half-ring configuration with  $(m_c + 1)$   $\beta'$ s; FRC: full-ring configuration with  $(2m_c + 1)$   $\beta'$ s; HFRC: full-ring configuration with  $(m_c + 1)$   $\beta'$ s. For odd  $m_c$  HFRC does not apply (CN goes to infinity).

different multiplicative factor for the elements coming from different  $B_\mu$ . If we denote  $C = \sum_\mu C(B_\mu)$  and the number of  $\beta'$ s added to  $B_\mu$  is  $\Delta n_\mu$ , then

$$C \mapsto \tilde{C} = \sum_{\mu, k} \frac{n_\mu + \Delta n_\mu}{n_\mu} P_k C(B_\mu) P_k.$$

If we choose  $\Delta n_\mu \propto n_\mu$  while guaranting  $n_\mu + \Delta n_\mu \geq 2m_c + 1$  for each  $\mu$ , the factor  $\frac{n_\mu + \Delta n_\mu}{n_\mu}$  becomes a global factor and can be factored out. The pinching argument goes through again and  $\kappa(\tilde{C}) \leq \kappa(C)$ . Thus we proved MFRC can give the optimal CN.

The reason why MFRC can have lower CN than FRC is due to the fact that sometimes  $\kappa(A) + \kappa(B) \geq \kappa(A + B)$  for matrices  $A$  and  $B$ . Note that since CN is a very complicated matrix function which is neither convex nor concave, the contrary can also be true for some  $A$  and  $B$ . Considering also the complicated structure of the covariance matrix here, it is often extremely difficult to figure out the true optimal configuration. However, we observed numerical evidence that the improvement of MFRC over the FRC with optimal ring radius is extremely small or even 0. Denote the covariance matrix for a ring of  $N_{m_c}$   $\beta'$ s with radius  $r$  as  $C_r$ . We compared  $\min_r \kappa(C_r)$  and  $\min_{r_1, r_2} \kappa(C_{r_1} + C_{r_2})$ . For  $m_c = 1$  we found a 1.6% difference and for  $m_c \geq 2$  they are equal. We thus conjecture that FRC is the optimal configuration for  $m_c \geq 2$ . Note that the number of  $\beta'$ s required for MFRC is at least twice as large as that of FRC. So practically FRC is much more efficient than MFRC.

#### Half-ring configuration approximates full-ring well

From the single-ring configurations, we find it possible to simplify FRC further. With less than  $(2m_c + 1)$  points, it is impossible to exactly satisfy  $\sum_j e^{i(k_1 - k_2)\phi_j} = \delta_{k_1 k_2}$  for all  $k_1, k_2$ . However, we find a very special asymptotic behavior of the covariance matrix, as stated by the following theorem (see appendix for the proof).

**Theorem 1.** *The large- $|\beta|$  asymptotic form of  $C_{m_1 m_2, m_3 m_4}(\beta)$  is*

$$C_{m_1 m_2, m_3 m_4}(\beta) \sim \begin{cases} g(m_1, m_2, m_3, m_4, \phi) / |\beta|, & \sum_{i=1}^4 m_i \text{ is even}; \\ g(m_1, m_2, m_3, m_4, \phi) / |\beta|^2, & \sum_{i=1}^4 m_i \text{ is odd}; \end{cases}$$

where  $\phi$  is the complex angle of  $\beta$ .

This theorem effectively says that the elements of  $C(\beta)$  has a “parity selection rule”.

So in the large  $|\beta|$  limit, the block  $C_{k_1 k_2} \sim 1/|\beta|$  if  $k_1 - k_2$  is even and  $C_{k_1 k_2} \sim 1/|\beta|^2$  if  $k_1 - k_2$  is odd. Certainly, all diagonal blocks  $C_{kk} \sim 1/|\beta|$ . So if  $|\beta|$  is large enough, the blocks with odd  $(k_1 - k_2)$  vanish even if we do not have FRC. To make the rest of the off-diagonal blocks vanish, we only need to choose a configuration such that  $\sum_j e^{i(k_1 - k_2)\phi_j} = \delta_{k_1 k_2}$  holds for even  $k_1 - k_2 = 2l$ , where  $l = 0, \pm 1, \pm 2, \dots, \pm m_c$ , i.e.

$$\sum_j e^{2il\phi_j} = \delta_{l,0}.$$

It is straightforward to check that the half-ring configuration (HRC),  $\phi_j = \frac{\pi}{m_c+1}j$  qualifies for all  $m_c$  and the “half of a full-ring” (HFRC),  $\phi_j = \frac{2\pi}{m_c+1}j$  qualifies for even  $m_c$ . In fact for even  $m_c$ ,  $\phi_j = \frac{2\pi n}{m_c+1}j$  could work for any non-zero integer  $n$ . Therefore if the optimal radius of FRC is large (which as we will show is usually the case), HRC should work equally well with only half of the measurements.

Another point to note is that the CN is insensitive to slight violation of the constraints, where the eigenvalues of  $\tilde{C}$  would be slightly perturbed. First, perturbation of the intermediate eigenvalues do not change CN. Note also that since  $\kappa(C) = \frac{\lambda_{max}(C)}{\lambda_{min}(C)}$ , CN is insensitive to perturbations of its denominator  $\lambda_{min}(C)$ . Slight perturbation to  $\lambda_{max}$  will only cause a small relative change because  $\lambda_{max}$  is a large number. Numerical calculation confirms our argument above, see Fig S4. As  $r = |\beta|$  increases, CN of HRC and HFRC (when it applies, i.e.  $m_c$  is even) quickly becomes indistinguishable with that of FRC. For  $m_c = 2$ , HFRC is slightly better in a small window of  $r$  and for  $m_c \geq 4$  HRC is generally better.

In numerical practice, we initialize the  $\beta'$ s according to many different schemes, start the gradient optimization of the CN, and pick the result that has the lowest CN. In most cases, the optimization starting with HRC gives the lowest CN and the final configuration given by the optimizer is pretty close to HRC. Cases with  $m_c \leq 2$  are more special. For  $m_c = 2$ , the best result is HFRC while for  $m_c = 1$ , the best result is similar to HRC but has a more significant deviation. Because for  $m_c = 1$ , unlike the other cases, the optimal radius of FRC does not occur in the large- $|\beta|$  regime and our previous argument does not really apply well here.

### Ring-based schemes for Homodyne tomography

Most of the above argument applies to Homodyne tomography as well. The term  $|m_1\rangle\langle m_2|$  contributes the Homodyne signal

$$\begin{aligned}\mathcal{H}(|m_1\rangle\langle m_2|) &= \text{tr}[|x_\theta\rangle\langle x_\theta| \cdot |m_1\rangle\langle m_2|] \\ &= \frac{e^{i(m_1-m_2)\theta}}{\pi^{1/2}\sqrt{2^{m_1+m_2}m_1!m_2!}} e^{-x^2} H_{m_1}(x) H_{m_2}(x).\end{aligned}$$

And the covariance matrix is

$$\begin{aligned}C_{m_1 m_2, m_3 m_4} &= \frac{e^{i(m_3-m_4-m_1+m_2)\theta}}{\pi\sqrt{2^{m_1+m_2+m_3+m_4}m_1!m_2!m_3!m_4!}} \int_{-\infty}^{+\infty} e^{-2x^2} H_{m_1}(x) H_{m_2}(x) H_{m_3}(x) H_{m_4}(x) \\ &\equiv \frac{e^{i(m_3-m_4-m_1+m_2)\theta}}{\pi\sqrt{2^{m_1+m_2+m_3+m_4}m_1!m_2!m_3!m_4!}} g(m_1, m_2, m_3, m_4).\end{aligned}$$

Due to the properties of the Hermite polynomials (i.e.  $H_n(x)$  is a odd/even function of  $x$  if  $n$  is odd/even), if  $m_1 + m_2 + m_3 + m_4$  is odd, the integral

$$\int_{-\infty}^{+\infty} dx e^{-2x^2} H_{m_1}(x) H_{m_2}(x) H_{m_3}(x) H_{m_4}(x) = 0.$$

To pinch the covariance matrix, we can use the half-ring configuration, i.e. pick  $(m_c + 1)$   $\theta_j$  such that  $\theta_j = \frac{\pi}{2m_c+1}j$  where  $j = 0, 1, 2, \dots, m_c$ .

Plugging definite values for  $m_1, m_2, m_3, m_4$ , we find the covariance matrix for Homodyne to be the same (up to constants) as the asymptotic covariance matrix for  $Q_n$  measurements.

### L. Comparison of $Q_n$ , Wigner and Homodyne tomography

Assuming only shot-noise, the figure of merit is  $\kappa(A)\sqrt{N_\beta}$ . For  $Q_n$  tomography,  $N_\beta$  is  $m_c + 1$  for HRC and  $2m_c + 1$  for FRC, both linear in  $m_c$ . Using the asymptotic expressions of the covariance matrix, we can calculate the CN of the asymptotic covariance matrix (which gives the optimal CN except for  $m_c = 1$ ). It turns out that the  $\kappa(A) \propto m_c^{1/2}$ , as shown in left panel of Fig S5. So  $\kappa(A)\sqrt{N_\beta} \sim m_c$ .

On the other hand, for Wigner tomography, we find a super-linear scaling of  $\kappa(A)\sqrt{N_\beta}$  with  $m_c$ , as shown in right panel of Fig. S5. Therefore as  $m_c$  gets larger the relative advantage of  $Q_n$  tomography with respect to Wigner tomography gets more significant. This is indeed the case, as demonstrated by the benchmarking results in Fig. S6.



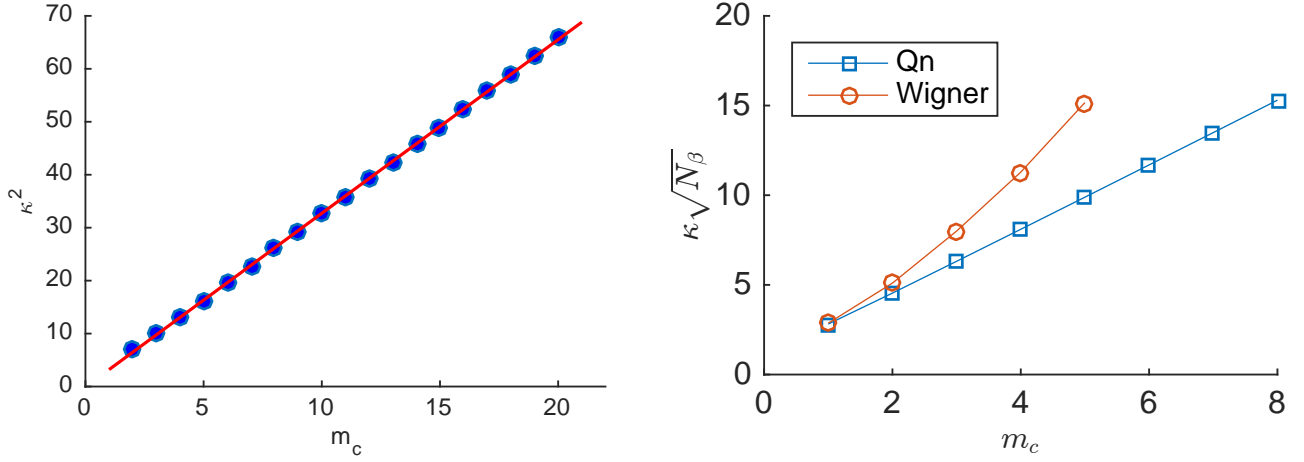


Figure S5. **Left Panel:** Optimal CN for  $Q_n$  measurements as a function of  $m_c$ . Vertical axis shows  $\kappa(A)^2$ . Red solid line shows a linear fit with equation  $\kappa^2 = 3.28m_c - 0.07769$ . **Right Panel:** Comparison of the figures of merits (assuming shot-noise only)  $\kappa\sqrt{N_\beta}$  for  $Q_n$  and Wigner tomography.

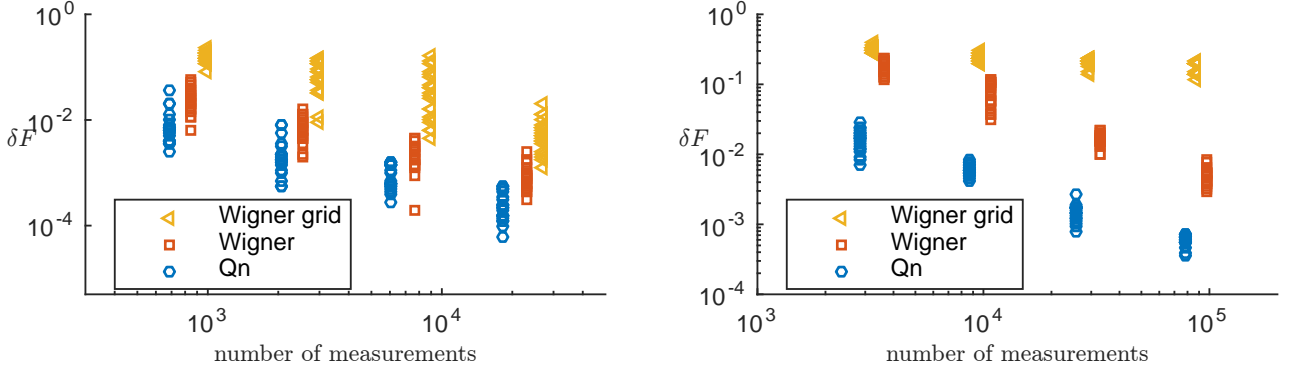


Figure S6. Benchmarking results with simulated data for  $m_c = 2$  and  $m_c = 5$ . The advantage of  $Q_n$  tomography becomes more significant as  $m_c$  increases, as expected.

### M. Generalized cat states reconstruction

As a generalization, we can also construct an optimized measurement set for the “generalized cat states”,  $\rho = \sum_{i,j,m_1,m_2} \rho_{i,m_1;j,m_2} |\alpha_i, m_1\rangle \langle \alpha_j, m_2|$ , where  $i, j = 1, 2, \dots, p$  and  $m_1, m_2 = 0, 1, \dots, m_c$ , and  $|\alpha_i, m_i\rangle \equiv D(\alpha_i)|m_i\rangle$  are displaced Fock states. Such states may arise when an ideal cat state state is subject to experimental noise and each coherent state component is deformed. Now each column of the sensing matrix has the form  $(d_i d_j e^{i\phi_{ij}})^n P(n)$  where  $P(n)$  is a polynomial coming from the associated Laguerre polynomials  $P(n) = \mathcal{L}_{m_1}^{n-m_1}(|\beta|^2) \mathcal{L}_{m_2}^{n-m_2}(|\beta|^2)$ . On a large scale of  $n$ , the change of  $(d_i d_j e^{i\phi_{ij}})^n P(n)$  as a function of  $n$  is dominated by the exponential part  $(d_i d_j e^{i\phi_{ij}})^n$ . So just as in the cat state case the columns with distinct  $d_i d_j e^{i\phi_{ij}}$  are linearly independent. For the  $(m_c + 1)^2$  columns that share the same  $d_i d_j e^{i\phi_{ij}}$  but different polynomials  $P(n)$ , we need  $(m_c + 1)$  different  $\beta$ 's to completely fix all unknowns as discussed previously. We can then run numerical optimization for all  $N \geq (m_c + 1)$  and pick the optimal  $N$  as done for the cat state case.

A simultaneous optimization of many  $\beta$ 's has the down side of easily getting stuck in local minima. Here we show an alternative greedy-policy for optimization that works pretty well, where we pick one best  $\beta$  at a time. The procedure is as follows. (1) Start with an empty set  $S = \emptyset$  of  $\beta$ 's, keeping all the  $\alpha$ 's but set  $m_c = 0$ , which allows the condition number to be finite with one  $\beta$ ; (2) Pick the optimal  $\beta$  (in the sense that it combined with those  $\beta$ 's in  $S$  produces the lowest condition number) and add it to the set  $S$ ; (3) If the optimal condition number is small enough, increase  $m_c$  by one (otherwise keep it the same); (4) Repeat (2) and (3) until one reaches the desired  $m_c$ .

We give one example here for which the condition number as a function of the next  $\beta$  to pick are shown in Fig. S7.

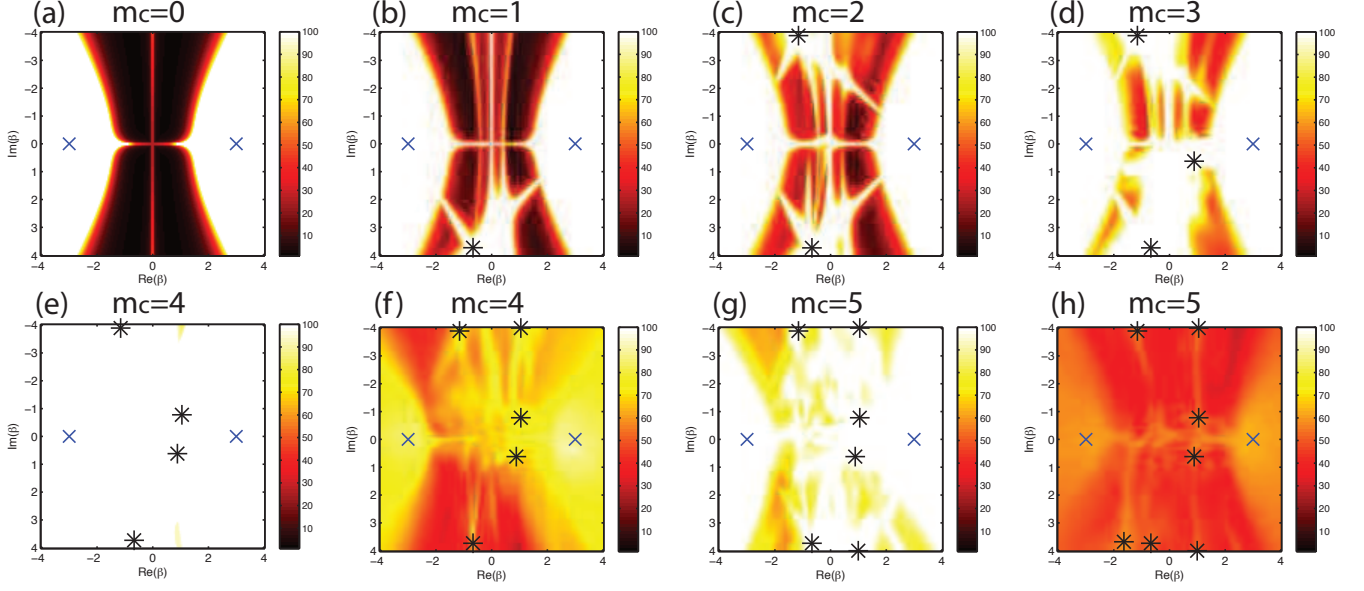


Figure S7. Step-by-step optimization of the set of  $\beta'$ s. Crosses show the position of  $\alpha'$ s and stars indicate all the  $\beta'$ s added to the set  $S$ . At each step, the optimal  $\beta$  is added to the set  $S$ . When the condition number is low enough (smaller than a preset threshold),  $m_c$  is increased by one and the optimization goes on.

## APPENDIX: PROOF OF THEOREM 1

For completeness, we provide the detailed proof of theorem 1 in this appendix.

**Theorem.** *The large- $|\beta|$  asymptotic form of  $C_{m_1 m_2, m_3 m_4}(\beta)$  is*

$$C_{m_1 m_2, m_3 m_4}(\beta) \sim \begin{cases} g(m_1, m_2, m_3, m_4, \phi) / |\beta|, & \sum_{i=1}^4 m_i \text{ is even}; \\ g(m_1, m_2, m_3, m_4, \phi) / |\beta|^2, & \sum_{i=1}^4 m_i \text{ is odd}; \end{cases}$$

where  $\phi$  is the complex angle of  $\beta$ .

### Some Preparation

**Lemma 2.** *Let  $I_\nu(z)$  denote the modified Bessel functions of the first kind. For any non-negative integer  $k$ , we have*

$$\begin{aligned} \frac{\partial^k}{\partial z^k} [(2\sqrt{z})^\nu I_\nu(2\sqrt{z})] &= 2^k [(2\sqrt{z})^{\nu-k} I_{\nu-k}(2\sqrt{z})], \\ \frac{\partial^k}{\partial z^k} [(2\sqrt{z})^{-\nu} I_\nu(2\sqrt{z})] &= 2^k [(2\sqrt{z})^{-(\nu+k)} I_{\nu+k}(2\sqrt{z})], \end{aligned}$$

*Proof.* These can be verified using the properties of  $I_\nu(z)$ . □

**Lemma 3.** *Let  $n, j_1, j_2, j_3, j_4$  be non-negative integers, we have*

$$\begin{aligned} & \sum_{n=0}^{\infty} \frac{z^n}{(n!)^2} \binom{n}{j_1} \binom{n}{j_2} \binom{n}{j_3} \binom{n}{j_4} \\ &= \frac{1}{j_1! j_2! j_3! j_4!} z^{j_4} \frac{\partial^{j_4}}{\partial z^{j_4}} z^{j_3} \frac{\partial^{j_3}}{\partial z^{j_3}} z^{j_2} \frac{\partial^{j_2}}{\partial z^{j_2}} z^{j_1} \frac{\partial^{j_1}}{\partial z^{j_1}} I_0(2\sqrt{z}) \\ &= \sum_{k_4=0}^{j_4} \sum_{k_3=0}^{j_3} \frac{j_4!}{k_4!(j_4-k_4)!} \frac{j_3!}{k_3!(j_3-k_3)!} \frac{j_2!}{(j_2-k_3)!} \frac{(j_2+j_3-k_3)!}{(j_2+j_3-k_3-k_4)!} (\sqrt{z})^{j_1+j_2+j_3+j_4-k_3-k_4} I_{j_1-j_2-j_3-j_4+k_3+k_4}(2\sqrt{z}). \end{aligned}$$

where  $I_0(2\sqrt{z}) = \sum_{n=0}^{\infty} \frac{z^n}{(n!)^2}$ .

*Proof.* It is straightforward to show tha

$$\sum_n \frac{z^n}{(n!)^2} \binom{n}{j} = \frac{1}{j!} \sum_n \frac{z^n}{(n!)^2} n(n-1) \cdots (n-j+1) = \frac{1}{j!} z^j \frac{\partial^j}{\partial z^j} I_0(2\sqrt{z}).$$

Similarly,

$$\sum_{n=0}^{\infty} \frac{z^n}{(n!)^2} \binom{n}{j_1} \binom{n}{j_2} \binom{n}{j_3} \binom{n}{j_4} = \frac{1}{j_1! j_2! j_3! j_4!} z^{j_4} \frac{\partial^{j_4}}{\partial z^{j_4}} z^{j_3} \frac{\partial^{j_3}}{\partial z^{j_3}} z^{j_2} \frac{\partial^{j_2}}{\partial z^{j_2}} z^{j_1} \frac{\partial^{j_1}}{\partial z^{j_1}} I_0(2\sqrt{z}).$$

We now try to express the above quantity in an explicit form.

First, using Lemma 2,

$$\frac{\partial^{j_1}}{\partial z^{j_1}} I_0(2\sqrt{z}) = 2^{j_1} [(2\sqrt{z})^{-j_1} I_{-j_1}(2\sqrt{z})].$$

Next,

$$\frac{\partial^{j_2}}{\partial z^{j_2}} z^{j_1} \frac{\partial^{j_1}}{\partial z^{j_1}} I_0(2\sqrt{z}) = 2^{j_2-j_1} [(2\sqrt{z})^{j_1-j_2} I_{j_1-j_2}(2\sqrt{z})].$$

Continuing this, we can get

$$\begin{aligned} \frac{\partial^{j_3}}{\partial z^{j_3}} z^{j_2} \frac{\partial^{j_2}}{\partial z^{j_2}} z^{j_1} \frac{\partial^{j_1}}{\partial z^{j_1}} I_0(2\sqrt{z}) &= 2^{j_2-j_1} \frac{\partial^{j_3}}{\partial z^{j_3}} z^{j_2} [(2\sqrt{z})^{j_1-j_2} I_{j_1-j_2}(2\sqrt{z})] \\ &= 2^{j_2-j_1} \sum_{k_3=0}^{j_3} \binom{j_3}{k_3} \frac{\partial^{k_3}}{\partial z^{k_3}} (z^{j_2}) \frac{\partial^{j_3-k_3}}{\partial z^{j_3-k_3}} [(2\sqrt{z})^{j_1-j_2} I_{j_1-j_2}(2\sqrt{z})] \\ &= 2^{j_3+j_2-j_1} \sum_{k_3=0}^{j_3} \binom{j_3}{k_3} \frac{\partial^{k_3}}{\partial z^{k_3}} (z^{j_2}) 2^{-k_3} [(2\sqrt{z})^{j_1-j_2-j_3+k_3} I_{j_1-j_2-j_3+k_3}(2\sqrt{z})] \end{aligned}$$

Eventually we obtain

$$\begin{aligned} & z^{j_4} \frac{\partial^{j_4}}{\partial z^{j_4}} z^{j_3} \frac{\partial^{j_3}}{\partial z^{j_3}} z^{j_2} \frac{\partial^{j_2}}{\partial z^{j_2}} z^{j_1} \frac{\partial^{j_1}}{\partial z^{j_1}} I_0(2\sqrt{z}) \\ &= \sum_{k_4=0}^{j_4} \sum_{k_3=0}^{j_3} \frac{j_4!}{k_4!(j_4-k_4)!} \frac{j_3!}{k_3!(j_3-k_3)!} \frac{j_2!}{(j_2-k_3)!} \frac{(j_2+j_3-k_3)!}{(j_2+j_3-k_3-k_4)!} (\sqrt{z})^{j_1+j_2+j_3+j_4-k_3-k_4} I_{j_1-j_2-j_3-j_4+k_3+k_4}(2\sqrt{z}). \end{aligned}$$

Note that in the above derivation, factors like

$$\frac{a!}{(a-b)!} = a(a-1)(a-2) \cdots (a-b+1)$$

are naturally interpreted as 0 if  $a < b$ . □

**Lemma 4.** Let  $m$  be a positive integer,

$$\sum_{i=0}^m (-1)^i \binom{m}{i} i^k = \begin{cases} 0, & \text{if } 0 \leq k < m; \\ (-1)^m m!, & \text{if } k = m; \\ (-1)^m m! \binom{m+1}{2}, & \text{if } k = m+1. \end{cases}$$

*Proof.* Let  $\alpha$  be any real number,

$$(1+\alpha)^m = \sum_{i=0}^m \alpha^i \binom{m}{i}.$$

We then have

$$\left(\alpha \frac{\partial}{\partial \alpha}\right)^k (1 + \alpha)^m = \sum_{i=0}^m i^k \alpha^i \binom{m}{i}.$$

For  $0 \leq k < m$ , the power of  $(1 + \alpha)$  is at least  $m - k$ , and consequently

$$\sum_{i=0}^m i^k (-1)^i \binom{m}{i} = \left(\alpha \frac{\partial}{\partial \alpha}\right)^k (1 + \alpha)^m \Big|_{\alpha=-1} = 0,$$

which proves the first part of the lemma.

We now prove the rest of the lemma. Since the operator  $\alpha \frac{\partial}{\partial \alpha}$  preserves the power of  $\alpha$ , we may write

$$\left(\alpha \frac{\partial}{\partial \alpha}\right)^k (1 + \alpha)^m = \sum_{\mu=0}^k c_{\mu}^{(k)} \alpha^{\mu} \frac{\partial^{\mu}}{\partial \alpha^{\mu}} (1 + \alpha)^m.$$

Then for  $k + 1$ ,

$$\begin{aligned} \left(\alpha \frac{\partial}{\partial \alpha}\right)^{k+1} (1 + \alpha)^m &= \alpha \frac{\partial}{\partial \alpha} \sum_{\mu=0}^k c_{\mu}^{(k)} \alpha^{\mu} \frac{\partial^{\mu}}{\partial \alpha^{\mu}} (1 + \alpha)^m \\ &= \sum_{\mu=1}^k (c_{\mu}^{(k)} \mu + c_{\mu-1}^{(k)}) \alpha^{\mu} \frac{\partial^{\mu}}{\partial \alpha^{\mu}} (1 + \alpha)^m + c_k^{(k)} \alpha^{k+1} \frac{\partial^{k+1}}{\partial \alpha^{k+1}} (1 + \alpha)^m \\ &\equiv: \sum_{\mu=1}^{k+1} c_{\mu}^{(k+1)} \alpha^{\mu} \frac{\partial^{\mu}}{\partial \alpha^{\mu}} (1 + \alpha)^m. \end{aligned}$$

Matching coefficients we have the relation

$$\begin{aligned} c_{k+1}^{(k+1)} &= c_k^{(k)}, \\ c_k^{(k+1)} &= c_k^{(k)} k + c_{k-1}^{(k)}. \end{aligned}$$

Obviously  $c_0^{(0)} = 1$ , so

$$c_k^{(k)} = 1,$$

and

$$\begin{aligned} c_k^{(k+1)} &= c_k^{(k)} k + c_{k-1}^{(k)} = k + (k-1) c_{k-1}^{(k-1)} + c_{k-2}^{(k-1)} = \frac{k(k+1)}{2} + c_0^{(1)} \\ &= \frac{k(k+1)}{2}. \end{aligned}$$

where the last step uses the property  $c_0^{(1)} = 0$ .

Therefore when  $k = m$ ,

$$\begin{aligned} \left(\alpha \frac{\partial}{\partial \alpha}\right)^m (1 + \alpha)^m \Big|_{\alpha=-1} &= \sum_{\mu=0}^m c_{\mu}^{(m)} \alpha^{\mu} \frac{\partial^{\mu}}{\partial \alpha^{\mu}} (1 + \alpha)^m \Big|_{\alpha=-1} = c_m^{(m)} \alpha^m \frac{\partial^m}{\partial \alpha^m} (1 + \alpha)^m \Big|_{\alpha=-1} \\ &= (-1)^m m!. \end{aligned}$$

When  $k = m + 1$ ,

$$\begin{aligned} \left(\alpha \frac{\partial}{\partial \alpha}\right)^{m+1} (1 + \alpha)^m \Big|_{\alpha=-1} &= \sum_{\mu=0}^{m+1} c_{\mu}^{(m+1)} \alpha^{\mu} \frac{\partial^{\mu}}{\partial \alpha^{\mu}} (1 + \alpha)^m \Big|_{\alpha=-1} = c_m^{(m+1)} \alpha^m \frac{\partial^m}{\partial \alpha^m} (1 + \alpha)^m \Big|_{\alpha=-1} \\ &= (-1)^m m! \binom{m+1}{2}. \end{aligned}$$

□

**Proof of Theorem 1**

*Proof.* Let  $\beta = |\beta| e^{i\phi}$ ,  $x \equiv |\beta|$ ,  $M = m_1 + m_2 + m_3 + m_4$ , we have

$$\begin{aligned} C_{m_1, m_2; m_3, m_4}(\beta) &= \sum_n A_{n; m_1 m_2}^* A_{n; m_3 m_4} \\ &= e^{i\phi(m_2 + m_3 - m_1 - m_4)} (-1)^M \sqrt{m_1! m_2! m_3! m_4!} x^{-M} e^{-2x^2} \\ &\quad \times \sum_n \frac{x^{4n}}{(n!)^2} \mathcal{L}_{m_1}^{n-m_1}(x^2) \mathcal{L}_{m_2}^{n-m_2}(x^2) \mathcal{L}_{m_3}^{n-m_3}(x^2) \mathcal{L}_{m_4}^{n-m_4}(x^2) \end{aligned}$$

Using the explicit formula for the associated Laguerre polynomial

$$\mathcal{L}_m^{n-m}(x^2) = \sum_{i=0}^m \frac{1}{i!} \binom{n}{m-i} (-x^2)^i = \sum_{j=0}^m \binom{n}{j} \frac{(-1)^{m-j}}{(m-j)!} x^{2(m-j)},$$

we find that

$$\begin{aligned} &\sum_n \frac{x^{4n}}{(n!)^2} \mathcal{L}_{m_1}^{n-m_1}(x^2) \mathcal{L}_{m_2}^{n-m_2}(x^2) \mathcal{L}_{m_3}^{n-m_3}(x^2) \mathcal{L}_{m_4}^{n-m_4}(x^2) \\ &= \sum_{j_1=0}^{m_1} \sum_{j_2=0}^{m_2} \sum_{j_3=0}^{m_3} \sum_{j_4=0}^{m_4} \frac{(-1)^{M-j_1-j_2-j_3-j_4} x^{2(M-j_1-j_2-j_3-j_4)}}{(m_1-j_1)! j_1! (m_2-j_2)! j_2! (m_3-j_3)! j_3! (m_4-j_4)! j_4!} \\ &\quad \times j_1! j_2! j_3! j_4! \sum_n \frac{x^{4n}}{(n!)^2} \binom{n}{j_1} \binom{n}{j_2} \binom{n}{j_3} \binom{n}{j_4} \end{aligned}$$

Letting  $z = x^4$ , using Lemma 3, we have

$$\begin{aligned} &j_1! j_2! j_3! j_4! \sum_n \frac{x^{4n}}{(n!)^2} \binom{n}{j_1} \binom{n}{j_2} \binom{n}{j_3} \binom{n}{j_4} \\ &= z^{j_4} \frac{\partial^{j_4}}{\partial z^{j_4}} z^{j_3} \frac{\partial^{j_3}}{\partial z^{j_3}} z^{j_2} \frac{\partial^{j_2}}{\partial z^{j_2}} z^{j_1} \frac{\partial^{j_1}}{\partial z^{j_1}} I_0(2\sqrt{z}) \\ &= \sum_{k_4=0}^{j_4} \sum_{k_3=0}^{j_3} \frac{j_4!}{k_4!(j_4-k_4)!} \frac{j_3!}{k_3!(j_3-k_3)!} \frac{j_2!}{(j_2-k_3)!} \frac{(j_2+j_3-k_3)!}{(j_2+j_3-k_3-k_4)!} (\sqrt{z})^{j_1+j_2+j_3+j_4-k_3-k_4} I_{j_1-j_2-j_3-j_4+k_3+k_4}(2\sqrt{z}). \end{aligned}$$

Therefore after some simplification

$$\begin{aligned} &\sum_n \frac{x^{4n}}{(n!)^2} \mathcal{L}_{m_1}^{n-m_1}(x^2) \mathcal{L}_{m_2}^{n-m_2}(x^2) \mathcal{L}_{m_3}^{n-m_3}(x^2) \mathcal{L}_{m_4}^{n-m_4}(x^2) \\ &= (-1)^M x^{2M} \sum_{j_1=0}^{m_1} \sum_{j_2=0}^{m_2} \sum_{j_3=0}^{m_3} \sum_{j_4=0}^{m_4} \frac{(-1)^{j_1+j_2+j_3+j_4}}{(m_1-j_1)! j_1! (m_2-j_2)! j_2! (m_3-j_3)! j_3! (m_4-j_4)! j_4!} \\ &\quad \times \sum_{k_4=0}^{j_4} \sum_{k_3=0}^{j_3} \frac{j_4!}{k_4!(j_4-k_4)!} \frac{j_3!}{k_3!(j_3-k_3)!} \frac{j_2!}{(j_2-k_3)!} \frac{(j_2+j_3-k_3)!}{(j_2+j_3-k_3-k_4)!} (x^2)^{-k_3-k_4} I_{j_1-j_2-j_3-j_4+k_3+k_4}(2x^2). \end{aligned}$$



Part of the above formula can be further simplified,

$$\begin{aligned}
& \sum_{j_3=0}^{m_3} \sum_{j_4=0}^{m_4} \frac{(-1)^{j_3+j_4}}{(m_3-j_3)!j_3!(m_4-j_4)!j_4!} \\
& \times \sum_{k_4=0}^{j_4} \sum_{k_3=0}^{j_3} \frac{j_4!}{k_4!(j_4-k_4)!} \frac{j_3!}{k_3!(j_3-k_3)!} \frac{j_2!}{(j_2-k_3)!} \frac{(j_2+j_3-k_3)!}{(j_2+j_3-k_3-k_4)!} (x^2)^{-k_3-k_4} I_{j_1-j_2-j_3-j_4+k_3+k_4}(2x^2) \\
& = \sum_{k_4=0}^{m_4} \sum_{k_3=0}^{m_3} \sum_{j_3=k_3}^{m_3} \sum_{j_4=k_4}^{m_4} \frac{(-1)^{j_3+j_4}}{(m_3-j_3)!(m_4-j_4)!} \\
& \times \frac{1}{k_4!(j_4-k_4)!} \frac{1}{k_3!(j_3-k_3)!} \frac{j_2!}{(j_2-k_3)!} \frac{(j_2+j_3-k_3)!}{(j_2+j_3-k_3-k_4)!} (x^2)^{-k_3-k_4} I_{j_1-j_2-j_3-j_4+k_3+k_4}(2x^2) \\
& = \sum_{k_4=0}^{m_4} \sum_{k_3=0}^{m_3} \sum_{j_3=0}^{m_3-k_3} \sum_{j_4=0}^{m_4-k_4} \frac{(-1)^{j_3+k_3+j_4+k_4}}{(m_3-j_3-k_3)!(m_4-j_4-k_4)!} \\
& \times \frac{1}{k_4!j_4!} \frac{1}{k_3!j_3!} \frac{j_2!}{(j_2-k_3)!} \frac{(j_2+j_3)!}{(j_2+j_3-k_4)!} (x^2)^{-k_3-k_4} I_{j_1-j_2-j_3-j_4}(2x^2) \\
& = \sum_{k_4=0}^{m_4} \sum_{k_3=0}^{m_3} \frac{(x^2)^{-k_3-k_4}}{k_3!k_4!} (-1)^{k_3+k_4} \frac{j_2!}{(j_2-k_3)!(m_3-k_3)!(m_4-k_4)!} \\
& \times \sum_{j_3=0}^{m_3-k_3} (-1)^{j_3} \frac{(j_2+j_3)!}{(j_2+j_3-k_4)!} \binom{m_3-k_3}{j_3} \sum_{j_4=0}^{m_4-k_4} (-1)^{j_4} \binom{m_4-k_4}{j_4} I_{j_1-j_2-j_3-j_4}(2x^2).
\end{aligned}$$

Now

$$\begin{aligned}
& \sum_n \frac{x^{4n}}{(n!)^2} \mathcal{L}_{m_1}^{n-m_1}(x^2) \mathcal{L}_{m_2}^{n-m_2}(x^2) \mathcal{L}_{m_3}^{n-m_3}(x^2) \mathcal{L}_{m_4}^{n-m_4}(x^2) \\
& = (-1)^M x^{2M} \frac{1}{m_1!m_2!} \sum_{k_4=0}^{m_4} \sum_{k_3=0}^{m_3} \frac{(x^2)^{-k_3-k_4}}{k_3!k_4!(m_3-k_3)!(m_4-k_4)!} (-1)^{k_3+k_4} \\
& \times \sum_{j_1=0}^{m_1} (-1)^{j_1} \binom{m_1}{j_1} \sum_{j_2=0}^{m_2} (-1)^{j_2} \binom{m_2}{j_2} \frac{j_2!}{(j_2-k_3)!} \\
& \times \sum_{j_3=0}^{m_3-k_3} (-1)^{j_3} \frac{(j_2+j_3)!}{(j_2+j_3-k_4)!} \binom{m_3-k_3}{j_3} \sum_{j_4=0}^{m_4-k_4} (-1)^{j_4} \binom{m_4-k_4}{j_4} I_{j_1-j_2-j_3-j_4}(2x^2).
\end{aligned}$$

We now focus on one term in the double summation  $\sum_{k_4=0}^{m_4} \sum_{k_3=0}^{m_3}$ , i.e. the summand with fixed  $k_3$  and  $k_4$ . It is known that for large  $z$ ,

$$I_\nu(z) \sim \frac{e^z}{\sqrt{2\pi z}} \left[ 1 - \frac{4\nu^2-1}{8z} + \frac{(4\nu^2-1)(4\nu^2-9)}{2!(8z)^2} + \dots + (-1)^l \frac{\prod_{i=1}^l [4\nu^2 - (2i-1)^2]}{l!(8z)^l} + \dots \right],$$

in our case

$$I_{j_1-j_2-j_3-j_4}(2x^2) \sim \frac{e^{2x^2}}{2x\sqrt{\pi}} \left[ 1 - \frac{4(j_1-j_2-j_3-j_4)^2-1}{16x^2} \dots + (-1)^l \frac{\prod_{i=1}^l [4(j_1-j_2-j_3-j_4)^2 - (2i-1)^2]}{l!(4x)^{2l}} + \dots \right].$$

The expansion of  $I_{j_1-j_2-j_3-j_4}(2x^2)$  contains polynomials of the form  $j_1^{p_1} j_2^{p_2} j_3^{p_3} j_4^{p_4}$ . Note also  $\frac{j_2!}{(j_2-k_3)!}$  is a polynomial of  $j_2$  of degree  $k_3$  and  $\frac{(j_2+j_3)!}{(j_2+j_3-k_4)!}$  is polynomial of  $(j_2+j_3)$  of degree  $k_4$ . So overall the summand of the quadruple summation  $\sum_{j_1=0}^{m_1} \sum_{j_2=0}^{m_2} \sum_{j_3=0}^{m_3-k_3} \sum_{j_4=0}^{m_4-k_4}$  is a combination of polynomials of the form  $j_1^{p_1} j_2^{p_2} j_3^{p_3} j_4^{p_4}$ . Due to Lemma 4, the terms  $j_1^{p_1} j_2^{p_2} j_3^{p_3} j_4^{p_4}$  that gives non-zero contribution are those with  $p_1 \geq m_1$ ,  $p_2 \geq m_2$ ,  $p_3 \geq m_3 - k_3$ , and  $p_4 \geq m_4 - k_4$ . We try to find such terms with the lowest power in  $\frac{1}{x}$ . That is to find the smallest  $l$  such that the

following expression

$$\frac{j_2!}{(j_2 - k_3)!} \frac{(j_2 + j_3)!}{(j_2 + j_3 - k_4)!} \prod_{i=1}^l [4(j_1 - j_2 - j_3 - j_4)^2 - (2i - 1)^2]$$

contains a term like  $j_1^{m_1} j_2^{m_2} j_3^{m_3 - k_3} j_4^{m_4 - k_4}$  or of even higher order. Since

$$\frac{j_2!}{(j_2 - k_3)!} \frac{(j_2 + j_3)!}{(j_2 + j_3 - k_4)!} \prod_{i=1}^l [4(j_1 - j_2 - j_3 - j_4)^2 - (2i - 1)^2] = j_2^{k_3} (j_2 + j_3)^{k_4} 4^l (j_1 - j_2 - j_3 - j_4)^{2l} + (\text{lower order terms}),$$

we must require

$$k_3 + k_4 + 2l \geq m_1 + m_2 + m_3 - k_3 + m_4 - k_4,$$

i.e.

$$2(l + k_3 + k_4) \geq m_1 + m_2 + m_3 + m_4 = M.$$

Thus the smallest  $l$  should be

$$l_* = \begin{cases} \frac{M}{2} - k_3 - k_4, & \text{if } M \text{ even;} \\ \frac{M+1}{2} - k_3 - k_4, & \text{if } M \text{ odd.} \end{cases}$$

So if we neglect terms that either gives zero contribution to the quadruple sum over  $j_i$  or are not of the leading order in  $\frac{1}{x}$ ,

$$\begin{aligned} & \frac{j_2!}{(j_2 - k_3)!} \frac{(j_2 + j_3)!}{(j_2 + j_3 - k_4)!} I_{j_1 - j_2 - j_3 - j_4}(2x^2) \\ & \sim j_2^{k_3} (j_2 + j_3)^{k_4} (-1)^{l_*} \frac{4^{l_*} (j_1 - j_2 - j_3 - j_4)^{2l_*}}{l_*! (4x)^{2l_*}} \frac{e^{2x^2}}{2x\sqrt{\pi}} \\ & = j_2^{k_3} (j_2 + j_3)^{k_4} (j_1 - j_2 - j_3 - j_4)^{2l_*} \frac{(-1)^{l_*}}{l_*! 4^{l_*} x^{2l_*}} \frac{e^{2x^2}}{2x\sqrt{\pi}}. \end{aligned}$$

**When  $M$  is even,**  $2(l_* + k_3 + k_4) = M$ , so

$$\begin{aligned} & \frac{j_2!}{(j_2 - k_3)!} \frac{(j_2 + j_3)!}{(j_2 + j_3 - k_4)!} I_{j_1 - j_2 - j_3 - j_4}(2x^2) \\ & \sim j_2^{k_3} \sum_{\mu=0}^{k_4} \binom{k_4}{\mu} j_2^\mu j_3^{(k_4 - \mu)} \\ & \quad \times (-1)^{m_2 + m_3 + m_4 - 2(k_3 + k_4)} j_1^{m_1} j_2^{m_2 - k_3 - \mu} j_3^{m_3 - k_3 - k_4 + \mu} j_4^{m_4 - k_4} \\ & \quad \times \left( \begin{matrix} M - 2k_3 - 2k_4 \\ m_1, m_2 - k_3 - \mu, m_3 - k_3 - k_4 + \mu, m_4 - k_4 \end{matrix} \right) \frac{(-1)^{l_*}}{l_*! 4^{l_*} x^{2l_*}} \frac{e^{2x^2}}{2x\sqrt{\pi}} \\ & = (-1)^{M - m_1} \sum_{\mu=0}^{k_4} \binom{k_4}{\mu} \left( \begin{matrix} M - 2k_3 - 2k_4 \\ m_1, m_2 - k_3 - \mu, m_3 - k_3 - k_4 + \mu, m_4 - k_4 \end{matrix} \right) j_1^{m_1} j_2^{m_2} j_3^{m_3 - k_3} j_4^{m_4 - k_4} \\ & \quad \times \frac{(-1)^{M/2 - k_3 - k_4}}{(M/2 - k_3 - k_4)! 2^{(M - 2k_3 - 2k_4)} x^{(M - 2k_3 - 2k_4)}} \frac{e^{2x^2}}{2x\sqrt{\pi}}, \end{aligned}$$

where  $\left( \begin{matrix} n \\ k_1, k_2, \dots, k_m \end{matrix} \right) \equiv \frac{n!}{k_1! k_2! \dots k_m!}$ .

Using Lemma 4,

$$\begin{aligned}
& \sum_{j_1=0}^{m_1} (-1)^{j_1} \binom{m_1}{j_1} \sum_{j_2=0}^{m_2} (-1)^{j_2} \binom{m_2}{j_2} \sum_{j_3=0}^{m_3-k_3} (-1)^{j_3} \binom{m_3-k_3}{j_3} \sum_{j_4=0}^{m_4-k_4} (-1)^{j_4} \binom{m_4-k_4}{j_4} j_1^{m_1} j_2^{m_2} j_3^{m_3-k_3} j_4^{m_4-k_4} \\
&= \sum_{j_1=0}^{m_1} (-1)^{j_1} \binom{m_1}{j_1} j_1^{m_1} \sum_{j_2=0}^{m_2} (-1)^{j_2} \binom{m_2}{j_2} j_2^{m_2} \sum_{j_3=0}^{m_3-k_3} (-1)^{j_3} \binom{m_3-k_3}{j_3} j_3^{m_3-k_3} \sum_{j_4=0}^{m_4-k_4} (-1)^{j_4} \binom{m_4-k_4}{j_4} j_4^{m_4-k_4} \\
&= (-1)^{M-k_3-k_4} m_1! m_2! (m_3-k_3)! (m_4-k_4)!.
\end{aligned}$$

Plugging back to the expression of  $\sum_n \frac{x^{4n}}{(n!)^2} \mathcal{L}_{m_1}^{n-m_1}(x^2) \mathcal{L}_{m_2}^{n-m_2}(x^2) \mathcal{L}_{m_3}^{n-m_3}(x^2) \mathcal{L}_{m_4}^{n-m_4}(x^2)$  we eventually get

$$\begin{aligned}
& \sum_n \frac{x^{4n}}{(n!)^2} \mathcal{L}_{m_1}^{n-m_1}(x^2) \mathcal{L}_{m_2}^{n-m_2}(x^2) \mathcal{L}_{m_3}^{n-m_3}(x^2) \mathcal{L}_{m_4}^{n-m_4}(x^2) \\
& \sim (-1)^{m_1+M/2} e^{2x^2} x^{M-1} \frac{1}{2^{M+1}} \frac{1}{\sqrt{\pi}} \sum_{k_4=0}^{m_4} \sum_{k_3=0}^{m_3} \frac{(-1)^{k_3+k_4} 2^{2(k_3+k_4)}}{k_3! k_4! (M/2 - k_3 - k_4)!} \\
& \quad \times \sum_{\mu=0}^{k_4} \binom{k_4}{\mu} \binom{M-2k_3-2k_4}{m_1, m_2-k_3-\mu, m_3-k_3-k_4+\mu, m_4-k_4}.
\end{aligned}$$

Finally, we have the leading order contribution for the even  $M$  case:

$$\begin{aligned}
C_{m_1, m_2; m_3, m_4}(\beta) & \sim x^{-1} e^{i\phi(m_2+m_3-m_1-m_4)} \sqrt{m_1! m_2! m_3! m_4!} (-1)^{m_1+M/2} \frac{1}{2^{M+1} \sqrt{\pi}} \\
& \quad \times \sum_{k_4=0}^{m_4} \sum_{k_3=0}^{m_3} \frac{(-1)^{k_3+k_4} 2^{2(k_3+k_4)}}{k_3! k_4! (M/2 - k_3 - k_4)!} \\
& \quad \times \sum_{\mu=0}^{k_4} \binom{k_4}{\mu} \binom{M-2k_3-2k_4}{m_1, m_2-k_3-\mu, m_3-k_3-k_4+\mu, m_4-k_4} \\
& = \frac{g(m_1, m_2, m_3, m_4, \phi)}{|\beta|}.
\end{aligned}$$

**When  $M$  is odd,**  $2(l_* + k_3 + k_4) = M + 1$ . In this case five terms give non-zero contribution under the quadruple sum of  $j_i$ , which are  $P_1 \equiv j_1^{m_1+1} j_2^{m_2} j_3^{m_3-k_3} j_4^{m_4-k_4}$ ,  $P_2 \equiv j_1^{m_1} j_2^{m_2+1} j_3^{m_3-k_3} j_4^{m_4-k_4}$ ,  $P_3 \equiv j_1^{m_1} j_2^{m_2} j_3^{m_3-k_3+1} j_4^{m_4-k_4}$ ,  $P_4 \equiv j_1^{m_1} j_2^{m_2} j_3^{m_3-k_3} j_4^{m_4-k_4+1}$  and  $P_5 \equiv j_1^{m_1} j_2^{m_2} j_3^{m_3-k_3} j_4^{m_4-k_4}$ .  $P_1, \dots, P_4$  are the highest order term about the variables  $j_i$  in the summand and  $P_5$  is the next highest order. Let us write

$$\frac{j_2!}{(j_2-k_3)!} \frac{(j_2+j_3)!}{(j_2+j_3-k_4)!} I_{j_1-j_2-j_3-j_4}(2x^2) \sim \frac{(-1)^{l_*}}{l_*! 4^{l_*} x^{2l_*}} \frac{e^{2x^2}}{2x\sqrt{\pi}} \sum_{\nu=1}^5 \lambda_\nu P_\nu.$$

The coefficients  $\lambda_\nu$  are essentially combinatoric factors and it is not difficult to work them out, although the process can be long and tedious. Eventually we find,

$$\lambda_1 = (-1)^{m_1+1} \sum_{\mu=0}^{k_4} \binom{k_4}{\mu} \binom{M+1-2k_3-2k_4}{m_1+1, m_2-k_3-\mu, m_3-k_3-k_4+\mu, m_4-k_4},$$

$$\lambda_2 = (-1)^{m_1} \sum_{\mu=0}^{k_4} \binom{k_4}{\mu} \binom{M+1-2k_3-2k_4}{m_1, m_2-k_3-\mu+1, m_3-k_3-k_4+\mu, m_4-k_4},$$

$$\lambda_3 = (-1)^{m_1} \sum_{\mu=0}^{k_4} \binom{k_4}{\mu} \binom{M+1-2k_3-2k_4}{m_1, m_2-k_3-\mu, m_3-k_3-k_4+\mu+1, m_4-k_4},$$

$$\begin{aligned}\lambda_4 &= (-1)^{m_1} \sum_{\mu=0}^{k_4} \binom{k_4}{\mu} \binom{M+1-2k_3-2k_4}{m_1, m_2-k_3-\mu, m_3-k_3-k_4+\mu, m_4-k_4+1}, \\ \lambda_5 &= \sum_{\mu=0}^{k_4} \frac{-k_3(k_3-1)}{2} \binom{k_4}{\mu} \binom{M+1-2k_3-2k_4}{m_1, m_2-k_3-\mu+1, m_3-k_3-k_4+\mu, m_4-k_4} \\ &\quad + \sum_{\mu=0}^{k_4-1} \frac{-k_4(k_4-1)}{2} \binom{k_4-1}{\mu} \binom{M+1-2k_3-2k_4}{m_1, m_2-k_3-\mu, m_3-k_3-k_4+\mu+1, m_4-k_4}.\end{aligned}$$

The **key point** to notice is that because  $2(l_* + k_3 + k_4) = M + 1$ , now the leading term in  $\frac{1}{x}$  is

$$\frac{(-1)^{l_*}}{l_*! 4^{l_*} x^{2l_*}} \frac{e^{2x^2}}{2x\sqrt{\pi}} = \frac{(-1)^{(M+1)/2-k_3-k_4}}{((M+1)/2-k_3-k_4)! 2^{(M+1-2k_3-2k_4)} x^{(M+1-2k_3-2k_4)}} \frac{e^{2x^2}}{2x\sqrt{\pi}} \sim \frac{1}{x^{(M+1-2k_3-2k_4)}} \frac{e^{2x^2}}{2x\sqrt{\pi}},$$

which is one order higher in  $\frac{1}{x}$  compared to the even  $M$  case.

Using Lemma 4,

$$\begin{aligned}& \sum_{j_1=0}^{m_1} (-1)^{j_1} \binom{m_1}{j_1} \sum_{j_2=0}^{m_2} (-1)^{j_2} \binom{m_2}{j_2} \sum_{j_3=0}^{m_3-k_3} (-1)^{j_3} \binom{m_3-k_3}{j_3} \sum_{j_4=0}^{m_4-k_4} (-1)^{j_4} \binom{m_4-k_4}{j_4} \sum_{\nu=1}^5 \lambda_\nu P_\nu \\ &= (-1)^{M-k_3-k_4} m_1! m_2! (m_3-k_3)! (m_4-k_4)! \\ &\quad \times \left[ \lambda_5 + \binom{m_1+1}{2} \lambda_1 + \binom{m_2+1}{2} \lambda_2 + \binom{m_3-k_3+1}{2} \lambda_3 + \binom{m_4-k_4+1}{2} \lambda_4 \right].\end{aligned}$$

Now

$$\begin{aligned}& \sum_n \frac{x^{4n}}{(n!)^2} \mathcal{L}_{m_1}^{n-m_1}(x^2) \mathcal{L}_{m_2}^{n-m_2}(x^2) \mathcal{L}_{m_3}^{n-m_3}(x^2) \mathcal{L}_{m_4}^{n-m_4}(x^2) \\ &\sim (-1)^{(M+1)/2} e^{2x^2} x^{M-2} \frac{1}{2^{M+2}\sqrt{\pi}} \sum_{k_4=0}^{m_4} \sum_{k_3=0}^{m_3} \frac{(-1)^{k_3+k_4} 2^{2(k_3+k_4)}}{k_3! k_4! ((M+1)/2-k_3-k_4)!} \\ &\quad \times \left[ \lambda_5 + \binom{m_1+1}{2} \lambda_1 + \binom{m_2+1}{2} \lambda_2 + \binom{m_3-k_3+1}{2} \lambda_3 + \binom{m_4-k_4+1}{2} \lambda_4 \right].\end{aligned}$$

Finally,

$$\begin{aligned}C_{m_1, m_2; m_3, m_4}(\beta) &\sim -x^{-2} e^{i\phi(m_2+m_3-m_1-m_4)} \sqrt{m_1! m_2! m_3! m_4!} (-1)^{(M+1)/2} \frac{1}{2^{M+2}\sqrt{\pi}} \\ &\quad \times \sum_{k_4=0}^{m_4} \sum_{k_3=0}^{m_3} \frac{(-1)^{k_3+k_4} 2^{2(k_3+k_4)}}{k_3! k_4! ((M+1)/2-k_3-k_4)!} \\ &\quad \times \left[ \lambda_5 + \binom{m_1+1}{2} \lambda_1 + \binom{m_2+1}{2} \lambda_2 + \binom{m_3-k_3+1}{2} \lambda_3 + \binom{m_4-k_4+1}{2} \lambda_4 \right] \\ &= \frac{g(m_1, m_2, m_3, m_4, \phi)}{|\beta|^2}.\end{aligned}$$

In summary, we have thus proved that for large  $|\beta|$ ,

$$C_{m_1 m_2, m_3 m_4}(\beta) \sim \begin{cases} g(m_1, m_2, m_3, m_4, \phi) / |\beta|, & \sum_{i=1}^4 m_i \text{ is even;} \\ g(m_1, m_2, m_3, m_4, \phi) / |\beta|^2, & \sum_{i=1}^4 m_i \text{ is odd;} \end{cases}$$

**NOTE:** In fact our technique can be used to prove the general asymptotic result

$$\sum_{n=0}^{\infty} \frac{1}{(n!)^2} x^{4n} \prod_i \mathcal{L}_{m_i}^{n-m_i}(x^2) \sim \begin{cases} x^{\sum_i m_i - 1}, & \sum_i m_i \text{ is even;} \\ x^{\sum_i m_i - 2}, & \sum_i m_i \text{ is odd.} \end{cases}$$

□

- 
- [1] D. Gross, Y.-K. Liu, S. T. Flammia, S. Becker, and J. Eisert, *Phys. Rev. Lett.* **105**, 150401 (2010).
  - [2] S. T. Flammia, D. Gross, Y.-K. Liu, and J. Eisert, *New Journal of Physics* **14**, 095022 (2012).
  - [3] A. Kalev, R. L. Kosut, and I. H. Deutsch, *Npj Quantum Information* **1**, 15018 EP (2015), article.
  - [4] G. Tóth, W. Wieczorek, D. Gross, R. Krischek, C. Schwemmer, and H. Weinfurter, *Phys. Rev. Lett.* **105**, 250403 (2010).
  - [5] C. Ferrie, *Phys. Rev. Lett.* **113**, 190404 (2014).
  - [6] D. H. Mahler, L. A. Rozema, A. Darabi, C. Ferrie, R. Blume-Kohout, and A. M. Steinberg, *Phys. Rev. Lett.* **111**, 183601 (2013).
  - [7] M. Cramer, M. B. Plenio, S. T. Flammia, R. Somma, D. Gross, S. D. Bartlett, O. Landon-Cardinal, D. Poulin, and Y.-K. Liu, *Nat Commun* **1**, 149 (2010).
  - [8] K. Vogel and H. Risken, *Phys. Rev. A* **40**, 2847 (1989).
  - [9] D. Sych, J. Řeháček, Z. Hradil, G. Leuchs, and L. L. Sánchez-Soto, *Phys. Rev. A* **86**, 052123 (2012).
  - [10] L. G. Lutterbach and L. Davidovich, *Phys. Rev. Lett.* **78**, 2547 (1997).
  - [11] P. Bertet, A. Auffeves, P. Maioli, S. Osnaghi, T. Meunier, M. Brune, J. M. Raimond, and S. Haroche, *Phys. Rev. Lett.* **89**, 200402 (2002).
  - [12] B. Vlastakis, G. Kirchmair, Z. Leghtas, S. E. Nigg, L. Frunzio, S. M. Girvin, M. Mirrahimi, M. H. Devoret, and R. J. Schoelkopf, *Science* **342**, 607 (2013).
  - [13] M. Hofheinz, H. Wang, M. Ansmann, R. C. Bialczak, E. Lucero, M. Neeley, A. D. O'Connell, D. Sank, J. Wenner, J. M. Martinis, and A. N. Cleland, *Nature* **459**, 546 (2009).
  - [14] S. Krastanov, V. V. Albert, C. Shen, C.-L. Zou, R. W. Heeres, B. Vlastakis, R. J. Schoelkopf, and L. Jiang, *Phys. Rev. A* **92**, 040303 (2015).
  - [15] R. W. Heeres, B. Vlastakis, E. Holland, S. Krastanov, V. V. Albert, L. Frunzio, L. Jiang, and R. J. Schoelkopf, *Phys. Rev. Lett.* **115**, 137002 (2015).
  - [16] M. Mirrahimi, Z. Leghtas, V. V. Albert, S. Touzard, R. J. Schoelkopf, L. Jiang, and M. H. Devoret, *New Journal of Physics* **16**, 045014 (2014).
  - [17] Z. Leghtas, S. Touzard, I. M. Pop, A. Kou, B. Vlastakis, A. Petrenko, K. M. Sliwa, A. Narla, S. Shankar, M. J. Hatridge, M. Reagor, L. Frunzio, R. J. Schoelkopf, M. Mirrahimi, and M. H. Devoret, *Science* **347**, 853 (2015).
  - [18] Z. Leghtas, G. Kirchmair, B. Vlastakis, R. J. Schoelkopf, M. H. Devoret, and M. Mirrahimi, *Phys. Rev. Lett.* **111**, 120501 (2013).
  - [19] N. Ofek, A. Petrenko, R. Heeres, P. Reinhold, Z. Leghtas, B. Vlastakis, Y. Liu, L. Frunzio, S. M. Girvin, L. Jiang, M. Mirrahimi, M. H. Devoret, and R. J. Schoelkopf, *nature*, accepted (2016).
  - [20] C. Wang, Y. Y. Gao, P. Reinhold, R. W. Heeres, N. Ofek, K. Chou, C. Axline, M. Reagor, J. Blumoff, K. M. Sliwa, L. Frunzio, S. M. Girvin, L. Jiang, M. Mirrahimi, M. H. Devoret, and R. J. Schoelkopf, *Science* **352**, 1087 (2016).
  - [21] B. Calkins, P. L. Mennea, A. E. Lita, B. J. Metcalf, W. S. Kolthammer, A. Lamas-Linares, J. B. Spring, P. C. Humphreys, R. P. Mirin, J. C. Gates, P. G. R. Smith, I. A. Walmsley, T. Gerrits, and S. W. Nam, *Opt. Express* **21**, 22657 (2013).
  - [22] S. Haroche and J.-M. Raimond, *Exploring the Quantum: Atoms, Cavities, and Photons* (Oxford University Press, New York, 2006).
  - [23] M. Brune, F. Schmidt-Kaler, A. Maali, J. Dreyer, E. Hagley, J. M. Raimond, and S. Haroche, *Phys. Rev. Lett.* **76**, 1800 (1996).
  - [24] C. Guerlin, J. Bernu, S. Deleglise, C. Sayrin, S. Gleyzes, S. Kuhr, M. Brune, J.-M. Raimond, and S. Haroche, *Nature* **448**, 889 (2007).
  - [25] H. Wang, M. Hofheinz, M. Ansmann, R. C. Bialczak, E. Lucero, M. Neeley, A. D. O'Connell, D. Sank, M. Weides, J. Wenner, A. N. Cleland, and J. M. Martinis, *Phys. Rev. Lett.* **103**, 200404 (2009).
  - [26] D. Leibfried, D. M. Meekhof, B. E. King, C. Monroe, W. M. Itano, and D. J. Wineland, *Phys. Rev. Lett.* **77**, 4281 (1996).
  - [27] S. An, J.-N. Zhang, M. Um, D. Lv, Y. Lu, J. Zhang, Z.-Q. Yin, H. T. Quan, and K. Kim, *Nat Phys* **11**, 193 (2015), article.
  - [28] H.-Y. Lo, D. Kienzler, L. de Clercq, M. Marinelli, V. Negnevitsky, B. C. Keitch, and J. P. Home, *Nature* **521**, 336 (2015), letter.
  - [29] G. Kirchmair, B. Vlastakis, Z. Leghtas, S. E. Nigg, H. Paik, E. Ginossar, M. Mirrahimi, L. Frunzio, S. M. Girvin, and R. J. Schoelkopf, *Nature* **495**, 205 (2013).
  - [30] T. Opatrný and D.-G. Welsch, *Phys. Rev. A* **55**, 1462 (1997).
  - [31] S. Mancini, P. Tombesi, and V. I. Man'ko, *EPL (Europhysics Letters)* **37**, 79 (1997).
  - [32] S. Deleglise, I. Dotsenko, C. Sayrin, J. Bernu, M. Brune, J.-M. Raimond, and S. Haroche, *Nature* **455**, 510 (2008).
  - [33] Unless there are additional constraints to  $\rho$  so that other methods like compressed sensing may apply.
  - [34] For the sake of simplicity here we assume the least square solution gives a physical  $\rho$ , and defer a more careful discussion based on semidefinite programming to Sec. A of [39].
  - [35] J. S. Lundeen, A. Feito, H. Coldenstrodt-Ronge, K. L. Pagnell, C. Silberhorn, T. C. Ralph, J. Eisert, M. B. Plenio, and I. A. Walmsley, *Nat Phys* **5**, 27 (2009).
  - [36] L. Zhang, H. B. Coldenstrodt-Ronge, A. Datta, G. Puentes, J. S. Lundeen, X.-M. Jin, B. J. Smith, M. B. Plenio, and I. A. Walmsley, *Nat Photon* **6**, 364 (2012).
  - [37] Actually, in some experiments the Wigner function was obtained from  $Q_n^\beta$  [13, 29].



- [38] Z. Leghtas, G. Kirchmair, B. Vlastakis, M. H. Devoret, R. J. Schoelkopf, and M. Mirrahimi, *Phys. Rev. A* **87**, 042315 (2013).
- [39] See supplementary material for details.
- [40] It is note-worthy that examples where tomography requires only one measurement setting is extremely rare.
- [41] This excludes some lines in phase space, lines connecting any pair of points  $(\alpha_i, \alpha_j)$  and the perpendicular bisector of the pair [39].
- [42] R. Bhatia, *Matrix Analysis* (Springer-Verlag, New York, 1997).
- [43] Y. I. Bogdanov, G. Brida, M. Genovese, S. P. Kulik, E. V. Moreva, and A. P. Shurupov, *Phys. Rev. Lett.* **105**, 010404 (2010).
- [44] A. Miranowicz, K. Bartkiewicz, J. Peřina, M. Koashi, N. Imoto, and F. Nori, *Phys. Rev. A* **90**, 062123 (2014).
- [45] A. Miranowicz, i. m. c. K. Özdemir, J. c. v. Bajer, G. Yusa, N. Imoto, Y. Hirayama, and F. Nori, *Phys. Rev. B* **92**, 075312 (2015).
- [46] For even  $m_c$ , the configuration  $\phi_j = \frac{2\pi}{m_c+1}j$ , for  $j = 0, 1, \dots, m_c$  works as well.
- [47] M. Grant and S. Boyd, “CVX: Matlab software for disciplined convex programming, version 2.1,” <http://cvxr.com/cvx> (2014).
- [48] M. Grant and S. Boyd, in *Recent Advances in Learning and Control*, Lecture Notes in Control and Information Sciences, edited by V. Blondel, S. Boyd, and H. Kimura (Springer-Verlag Limited, 2008) pp. 95–110, [http://stanford.edu/~boyd/graph\\_dcp.html](http://stanford.edu/~boyd/graph_dcp.html).
- [49] W. Chen, J. Hu, Y. Duan, B. Braverman, H. Zhang, and V. Vuletić, *Phys. Rev. Lett.* **115**, 250502 (2015).
- [50] A. I. Lvovsky, *Journal of Optics B: Quantum and Semiclassical Optics* **6**, S556 (2004).